



# Thrombin Receptor-Activating Peptides (TRAPs): Investigation of Bioactive Conformations via Structure–Activity, Spectroscopic, and Computational Studies

Marco A. Ceruso,<sup>a</sup> David F. McComsey,<sup>a</sup> Gregory C. Leo,<sup>a</sup> Patricia Andrade-Gordon,<sup>a</sup> Michael F. Addo,<sup>a</sup> Robert M. Scarborough,<sup>b</sup> Donna Oksenberg<sup>b</sup> and Bruce E. Maryanoff<sup>a,\*</sup>

<sup>a</sup>The R. W. Johnson Pharmaceutical Research Institute, Spring House, PA 19477, USA

<sup>b</sup>COR Therapeutics, Inc., South San Francisco, CA 94080, USA

Received 11 December 1998; accepted 10 May 1999

**Abstract**—The thrombin receptor (PAR-1) is an unusual transmembrane G-protein coupled receptor in that it is activated by serine protease cleavage of its extracellular N-terminus to expose an agonist peptide ligand, which is tethered to the receptor itself. Synthetic peptides containing the agonist motif, such as SFLLRN for human PAR-1, are capable of causing full receptor activation. We have probed the possible bioactive conformations of thrombin receptor-activating peptides (TRAPs) by systematic introduction of certain conformational perturbations, involving  $\alpha$ -methyl, ester  $\Psi(\text{COO})$ , and reduced-amide  $\Psi(\text{CH}_2\text{N})$  scans, into the minimum-essential agonist sequence (SFLLR) to probe the importance of the backbone conformation and amide NH hydrogen bonding. We performed extensive conformational searches of representative pentapeptides to derive families of putative bioactive structures. In addition, we employed <sup>1</sup>H NMR and circular dichroism (CD) to characterize the conformational disposition of certain pentapeptide analogues experimentally. Activation of platelet aggregation by our pentapeptide analogues afforded a structure-function correlation for PAR-1 agonist activity. This correlation was assisted by PAR-1 receptor binding data, which gauged the affinity of peptide ligands for the thrombin receptor independent of a functional cellular response derived from receptor activation (i.e. a pure molecular recognition event). Series of alanine-, proline-, and N-methyl-scan peptides were also evaluated for comparison. Along with the known structural features for PAR-1 agonist peptides, our work adds to the understanding of peptide topography relative to platelet functional activity and PAR-1 binding. The absolute requirement of a positively charged N-terminus for strong agonist activity was contradicted by the N-terminal hydroxyl peptide  $\Psi(\text{HO})\text{S-FLLR-NH}_2$ . The amide nitrogen between residues 1 and 2 was found to be a determinant of receptor recognition and the carbonyl groups along the backbone may be involved in hydrogen bonding with the receptor. Position 3 (P3) of TRAP-5 is known to tolerate a wide variety of side chains, but we also found that the amide nitrogen at this position can be substituted by an oxygen, as in SF- $\Psi(\text{COO})\text{-LLR-NH}_2$ , without diminishing activity. However, this peptide bond is sensitive to conformational changes in that SFPLR-NH<sub>2</sub> was active, whereas SF-NMeL-LR-NH<sub>2</sub> was not. Additionally, we found that position 3 does not tolerate rigid spacers, such as 3-aminocyclohexane-1-carboxylic acid and 2-aminocycloalkane-1-carboxylic acid, as analogues **1A**, **1B**, **2A**, **2B**, **3**, **4**, **5A** and **5B** lack agonist activity. On the basis of our results, we suggest that an extended structure of the agonist peptide is principally responsible for receptor recognition (i.e. binding) and that hydrophobic contact may occur between the side chains of the second (Phe) and fourth (Leu) residues (i.e. P2-P4 interaction). © 1999 Elsevier Science Ltd. All rights reserved.

## Introduction

Many biological processes rely on receptor-based intracellular communication involving endogenous hormones, neurotransmitters, or growth factors. Of particular significance are the G-protein coupled receptors (GPCRs), a large superfamily of cell-surface glycoproteins. GPCRs are activated by diverse small and large molecules, ranging from biogenic amines, such as dopamine and histamine, to peptides, such as substance P and cholecystokinin, to proteins, such as gonadotropin-releasing hormone (GnRH), and are also targets

Abbreviations: Nonstandard chemical abbreviations not defined in text: Boc, *tert*-butyloxycarbonyl; BOP-Cl, *N,N'*-bis(2-oxo-3-oxazolidinyl)phosphinyl chloride; DMS, dimethylsulfide; DMAP, 4-(dimethylamino)pyridine; DCE, 1,2-dichloroethane; DIC, *N,N'*-diisopropylcarbodiimide; PMC, 2,2,5,7,8-pentamethylchroman-6-sulfonyl; Mts, 2,4,6-trimethylbenzenesulfonyl; Fmoc, 9-fluorenylmethoxycarbonyl; HOBT, 1-hydroxybenzotriazole; TFA, trifluoroacetic acid; Har = homoarginine, Aib = L-2-aminoisobutyric acid; Cha = L-cyclohexylalanine.

Key words: Peptides; receptor agonists; NMR; circular dichroism; molecular modeling.

\* Corresponding author. Tel.: +1-215-628-5530; fax: +1-215-628-4985; e-mail: bmaryanoff@prius.nj.com

responsible for the action of a broad selection of drugs.<sup>1–6</sup> For a long time, all GPCRs were thought to be activated by native ligands, which are biosynthesized at a site remote from the receptor and compelled to travel some distance before reaching their target. However, this picture changed dramatically with the cloning of the “platelet” thrombin receptor (TR; PAR-1) from human megakaryocytoblastoma cells.<sup>7</sup> This unusual GPCR mediates the cellular actions of the serine protease  $\alpha$ -thrombin via *proteolytic cleavage* of its lengthy, extracellular, N-terminal peptide chain, between Arg-41 and Ser-42, to expose a new N-terminus bearing the sequence SFLLRN (TR 42-47).<sup>7–13</sup> Remarkably, synthetic peptides containing this motif, such as the hexapeptide SFLLRN-NH<sub>2</sub> (TRAP-6), exhibit full agonist properties for thrombin receptor activation independent of thrombin-induced proteolysis, indicating that the receptor-linked SFLLRN sequence does serve as an activating ligand.<sup>7,14</sup> Thus, the thrombin receptor became the *first known GPCR to be activated by a protease* (“protease-activated receptor” or “PAR”) and *the first GPCR to have an intramolecular mechanism for ligand activation*, in this case via a “tethered-peptide” epitope. Subsequently, three other members of this unique class of GPCRs, PAR-2, PAR-3, and PAR-4, have been identified.<sup>15–20</sup>

Systematic structure–activity studies in different laboratories have established several critical components of the thrombin receptor-activating peptides (TRAPs), relative to PAR-1.<sup>13,14,21–27</sup> The minimum sequence length is five amino acids, with SFLLR-NH<sub>2</sub> (TRAP-5) being a good agonist but SFLL-NH<sub>2</sub> being quite weak.<sup>14,21–24</sup> The phenylalanine (F) residue at position 2 is crucial for activity, while an N-terminal free amino group, a basic or aromatic residue at position 5, and a bulky aliphatic residue at position 4 are moderately important.<sup>14,22–26</sup> The amino acids at positions 1, 3, and 6 (S, L, and N, respectively) can be replaced by alanine without significantly attenuating agonist potency (“alanine scan”), positions 3 and 6 are highly tolerant of diverse substitution, and positions 1 and 3 tolerate substitution with proline (“proline scan”).<sup>14,22–27</sup> By contrast, the scanning of positions 1 through 5 with D- or N-Me amino acids caused a major loss in agonist potency.<sup>25,26,28</sup> Interestingly, modification of certain side chains, especially by having *p*-fluorophenylalanine at position 2, yielded agonist peptides with a significant enhancement of potency, such as A-(*p*-fluoro-F)-R-Cha-Har-Y-NH<sub>2</sub> and S-(*p*-fluoro-F)-Cha-Cha-RK-NH<sub>2</sub>.<sup>25,27,29,30</sup> The body of existing structure–activity data for TRAPs is based on functional biological activity mediated by the PAR-1 thrombin receptor, rather than on ligand binding affinity, and focuses mainly on the nature of the amino acid side chains of the peptides. However, for such peptide ligands it would be important to have receptor binding data to better correlate biological activity with structural features, such as backbone conformation and amide hydrogen-bonding. Thus, we were intent on obtaining PAR-1 receptor binding data.

A limited number of studies have been conducted to define the favored or bioactive conformations of TRAPs. In an NMR study of SFLLRN-containing

peptides, the 14-mer SFLLRNPNDKYEPF-NH<sub>2</sub> (TR 42-55; TRAP-14) was found to contain a stabilized turn between positions 6 and 9 (NPND), but the five N-terminal residues were unstructured in solution.<sup>31</sup> An NMR study of SFLLRNPNDKY-NH<sub>2</sub> (TR 42-52; TRAP-11) showed a central type-I  $\beta$ -turn around NPND that is controlled by the rigidity of the proline and the charge of the aspartyl residue.<sup>32</sup> Additionally, an unconstrained computational search of TRAP-6 revealed that this small peptide is capable of adopting a folded conformation involving a  $\gamma$ -turn around Leu-3;<sup>32</sup> however, this secondary structure type would not be stable in a polar hydrogen-bonding environment. A structural investigation of TRAP-6 analogues with various conformational perturbations at positions 1–3 (P1–P3) illustrated some salient points for a bioactive structure: (1) the Phe-2 side chain has a limited conformation with backbone torsional angles of an extended conformation; (2) the Leu-3 residue has a  $\phi$  torsional angle similar to that of proline and a  $\psi$  torsional angle close to that of a  $\beta$ -sheet; and (3) a *trans* configuration is likely for the amide bonds of S-F and F-L.<sup>28</sup> These studies, although quite valuable, have mainly addressed the conformational preference of the *unbound* ligand, rather than the *bound* bioactive form.

We have been interested in analyzing the possible bioactive conformations of TRAPs as part of a project directed toward the discovery of thrombin receptor (PAR-1) antagonists, a class of agents that could serve as useful antithrombotic drugs. Consequently, we have examined the effects of systematic introduction of conformational perturbations into the native agonist peptide sequence. In particular, we carried out  $\alpha$ -methyl, ester  $\Psi$ (COO), and reduced amide  $\Psi$ (CH<sub>2</sub>N) scans with SFLLR-NH<sub>2</sub> to assess the importance of the backbone conformation and amide NH hydrogen bonding. By using spatial constraints established for Phe-2 in the work of Shimamoto et al.<sup>28</sup> we performed extensive conformational searches of these and related pentapeptide structures to derive families of putative bioactive conformations. We employed <sup>1</sup>H NMR and circular dichroism (CD) measurements to characterize the conformational disposition of certain agonist peptide analogues experimentally. Activation of platelet aggregation by our pentapeptide analogues afforded a structure–function correlation for agonist activity, which was assisted by data from a novel PAR-1 receptor binding assay.<sup>33</sup> This allowed us to assess the affinity of agonist peptide ligands for PAR-1 independent of a functional cellular response derived from receptor activation, which is preferable for interpreting molecular recognition events. Our work adds to the body of information on the structure–function properties of TRAPs, and could help in the design of new agonist and antagonist molecules for PAR-1.

## Results

Considerable work with TRAPs, as noted above, has principally focused on the role of the individual side chains and of the termini. In this paper, we have taken a systematic approach to evaluating the spatial relationships between different elements of TRAP-5, by using a

three-pronged strategy. (1) TRAP-5 analogues that contain peptide-bond surrogates and local conformational perturbations were synthesized and biologically evaluated. Thus, we have analyzed  $\alpha$ -methyl, *N*-methyl, and proline scans of SFLLR-NH<sub>2</sub> to determine the influence of the peptide backbone conformation. Additionally, the importance of amide NH and carbonyl groups, potentially reflective of hydrogen bonding capabilities, was probed by replacing each peptide bond of SFLLR-NH<sub>2</sub> with ester (COO) and secondary amine (CH<sub>2</sub>NH) linkages. (2) The conformational space of relevant TRAP-5 mimetics was characterized computationally by using molecular dynamics methods. Thus, we performed extensive conformational searches of TRAP-5 and related pentapeptide structures to derive families of putative bioactive conformations. (3) The proposed three-dimensional models were tested by the synthesis, biological evaluation, and physical (<sup>1</sup>H NMR and CD) characterization of additional analogues. The biological responses of the synthetic peptides were measured by two independent methods: a functional cellular assay involving platelet aggregation and a PAR-1 binding assay<sup>33</sup> based on the very potent agonist ligand [<sup>3</sup>H]S-(*p*-fluoro-F)-Har-L-Har-KY-NH<sub>2</sub>. This dual evaluation is important in that the differential analysis of responses can distinguish those features in TRAP-5 analogues required for receptor recognition (binding) and signal transduction from those required for just receptor recognition. Reported structure-function relationships for diverse TRAP analogues have relied mainly on biological function mediated by PAR-1, which reflects both binding and subsequent signal transduction. Hence, our structure-activity results should be amenable for interpreting molecular recognition events of the PAR-1 ligands.

For SFLLR-NH<sub>2</sub> (TRAP-5), PAR-1 binding (IC<sub>50</sub> = 1.5  $\mu$ M) and platelet activation data (EC<sub>50</sub> = 0.49  $\mu$ M) are reasonably consistent (Table 1, entry 1). To check the binding assay against the functional assay further, we obtained a set of data for the alanine-scan peptides of TRAP-5 (entries 2–6). The results for alanine substitution at positions 1–4 are reasonably consistent with a correlation between receptor binding and platelet activation, although the agonist activity for SFLLA-NH<sub>2</sub> (entry 6) is weaker than one would expect from the level of receptor binding. In some cases, a correspondence between the receptor binding and agonist activity may be confounded by the presence of antagonist activity, which is determined as an IC<sub>50</sub> value for inhibition of thrombin-induced platelet aggregation or percent inhibition at 50  $\mu$ M. Indeed, SFLLA-NH<sub>2</sub> exhibits PAR-1 antagonism with an IC<sub>50</sub> value of 20  $\mu$ M. Consequently, it is probably unreasonable to expect a precise correspondence between the receptor binding and PAR-1 agonist data, although the binding data would generally be reliable in reflecting agonist or antagonist activity. Certainly, the functional result for replacement of F by A is consistent with the literature, and our binding result follows suit.

### Synthetic peptides and biological activity

The rational design of peptide ligands with specific biological activity requires knowledge about the topographical

**Table 1.** Biological data for TRAP-5 analogues containing peptide bond surrogates

Entry	Peptide	Platelet aggregation <sup>a</sup> EC <sub>50</sub> ( $\mu$ M)	Receptor binding <sup>b</sup> IC <sub>50</sub> ( $\mu$ M)
1	SFLLR-NH <sub>2</sub>	0.49 $\pm$ 0.08	1.5 $\pm$ 0.5
2	AFLLR-NH <sub>2</sub>	0.74 $\pm$ 0.16	0.66 $\pm$ 0.15
3	SALLR-NH <sub>2</sub>	> 50 (10%)	> 100
4	SFALR-NH <sub>2</sub>	1.2 $\pm$ 0.3	0.75 $\pm$ 0.2
5	SFLAR-NH <sub>2</sub>	3.4 $\pm$ 0.3	1.8 $\pm$ 0.8
6	SFLLA-NH <sub>2</sub>	34 $\pm$ 7 <sup>c</sup>	1.7 $\pm$ 0.7
7	$\Psi$ (HO)A-FLLR-NH <sub>2</sub>	3.3 $\pm$ 0.7	14
8	$\Psi$ (HO)S-FLLR-NH <sub>2</sub>	3.7 $\pm$ 0.4	3.6
9	S- $\Psi$ (COO)-FLLR-NH <sub>2</sub>	> 50 (20%)	> 100
10	SF- $\Psi$ (COO)-LLR-NH <sub>2</sub>	0.24 $\pm$ 0.18	8.9 $\pm$ 4.1
11	SFL- $\Psi$ (COO)-LR-NH <sub>2</sub>	> 50 (38%)	20
12	SFLL- $\Psi$ (COO)-R-NH <sub>2</sub>	> 50 (31%)	2.5
13	S- $\Psi$ (CH <sub>2</sub> NH)-FLLR-NH <sub>2</sub>	> 50 (5%)	> 100
14	SF- $\Psi$ (CH <sub>2</sub> NH)-LLR-NH <sub>2</sub>	> 50 (7%)	> 100
15	SFL- $\Psi$ (CH <sub>2</sub> NH)-LR-NH	> 50 (11%)	> 100
16	SFLL- $\Psi$ (CH <sub>2</sub> NH)-R-NH	> 50 (17%)	> 100

<sup>a</sup> Activation of human platelet aggregation, expressed as an EC<sub>50</sub> value in  $\mu$ M, or percent aggregation induced at 50  $\mu$ M. PAR-1 antagonist activity was not significant (< 20% at 50  $\mu$ M), unless noted otherwise.

<sup>b</sup> Inhibition of radiolabeled agonist peptide binding to PAR-1, expressed as an IC<sub>50</sub> value in  $\mu$ M. IC<sub>50</sub> values are the concentration of test ligand required for 50% inhibition of the radioligand (*n* = 3 when the error limits are given; otherwise, *n* = 1).

<sup>c</sup> Antagonist IC<sub>50</sub> value of 20  $\mu$ M.

and geometrical properties associated with ligand recognition and receptor activation. In our structure-function studies, topographical features were probed by replacing backbone atoms (Table 1) and conformational attributes were probed by impacting the flexibility of the peptide backbone (Table 2). To investigate the backbone elements possibly involved in hydrogen-bonding interactions, either within TRAP-5 (intramolecular) or with the receptor (intermolecular), we synthesized and bioassayed two series of pentapeptides: an ester linkage scan series, employing  $\Psi$ (COO) for each amide linkage (depsipeptides) and a reduced-amide scan series, employing the amide-bond surrogate  $\Psi$ (CH<sub>2</sub>NH). Deletion of carbonyl groups along the backbone produced compounds that did not bind to PAR-1 and, correspondingly, there was no functional response observed (Table 1). On the other hand, most of the depsipeptides were capable of eliciting at least one of the two biological responses. Of particular note, SF- $\Psi$ (COO)-LLR-NH<sub>2</sub> (Table 1, entry 10) showed response levels comparable to those of TRAP-5. However, SFL- $\Psi$ (COO)-LR-NH<sub>2</sub> and SFLL- $\Psi$ (COO)-R-NH<sub>2</sub> (entries 11 and 12), although capable of binding, failed to induce platelet aggregation; also, S- $\Psi$ (COO)-FLLR-NH<sub>2</sub> (entry 9) was devoid of activity. Among the depsipeptide analogues, we prepared a derivative with L-glyceric acid in place of Ser-1,  $\Psi$ (HO)S-FLLR-NH<sub>2</sub> (entry 8), and this compound was capable of PAR-1 binding and activation. This is surprising because the positively charged N-terminus is now replaced by a neutral hydroxyl. To test this observation further, the L-lactic acid analogue,  $\Psi$ (HO)A-FLLR-NH<sub>2</sub> (entry 7), was prepared and found to be comparable in activity to the L-glyceric acid compound. The data for the  $\Psi$ (COO)

**Table 2.** Biological data for conformationally restricted TRAP-5 analogues

Entry	Peptide	Platelet aggregation <sup>a</sup> EC <sub>50</sub> (μM)	Receptor binding <sup>b</sup> IC <sub>50</sub> (μM)
1	SFLLR-NH <sub>2</sub>	0.49 ± 0.08	1.5 ± 0.5
2	NMeS-FLLR-NH <sub>2</sub>	16 ± 4 <sup>c</sup>	0.7 ± 0.3
3	S-NMeF-LLR-NH <sub>2</sub>	> 50 (3%)	62 ± 9
4	SF-NMeL-LR-NH <sub>2</sub>	> 50 (10%)	5.3 ± 0.7
5	SFL-NMeL-R-NH <sub>2</sub>	> 50 (12%)	16 ± 0.8
6	SFLL-NMeR-NH <sub>2</sub>	> 50 (37%)	11 ± 4
7	αMeS-FLLR-NH <sub>2</sub>	> 50 (10%)	> 100
8	S-αMeF-LLR-NH <sub>2</sub>	> 50 (10%)	> 100
9	SF-αMeL-LR-NH <sub>2</sub> <sup>d</sup>	> 50 (18%)	> 100
10	SFL-αMeL-R-NH <sub>2</sub> <sup>d</sup>	> 50 (17%)	> 100
11	SFLL-αMeR-NH <sub>2</sub>	> 50 (17%)	> 100
12	PFLLR-NH <sub>2</sub>	0.59 ± 0.14	0.52 ± 0.15
13	SPLLR-NH <sub>2</sub>	> 50 (3%)	> 100
14	SFPLR-NH <sub>2</sub>	4.1 ± 0.5 <sup>e</sup>	1.7 ± 0.2
15	SFLPR-NH <sub>2</sub>	> 50 (4%)	52 ± 8
16	SFLLP-NH <sub>2</sub>	> 50 (11%)	14 ± 4

<sup>a</sup> See Table 1.<sup>b</sup> See Table 1.<sup>c</sup> Antagonist IC<sub>50</sub> value of 39 ± 2.5 μM.<sup>d</sup> 1:1 Mixture of diastereomers due to racemic αMeL.<sup>e</sup> Antagonist IC<sub>50</sub> value of ca. 50 μM.

and Ψ(CH<sub>2</sub>NH) analogues suggest that all of the backbone carbonyls are essential for recognition at the receptor surface of PAR-1 and that at least a subset of amide protons participate in intramolecular or intermolecular hydrogen bonding (see Discussion).

Next, we deliberately perturbed the conformation of each residue along the sequence to investigate the backbone geometry of TRAP-5 as it binds to or activates the receptor. Addition of a methyl group to the α-carbon (α-methyl scan) or to the amide nitrogen (*N*-methyl scan) is expected to reorient the local conformation at the modified residue.<sup>34–37</sup> In the case of *N*-methyl substitution, the conformation of the preceding residue (i.e. that toward the N-terminal) will also be affected. However, in such alterations conformational control is gained through introduction of steric bulk, which needs to be taken into account when interpreting the results. Besides conducting α-methyl and *N*-methyl scans with TRAP-5, we also conducted a proline scan, although this one may have a disadvantage because of mutating the side chain of the residue under study (Table 2). The only conformationally perturbed analogues with activity in the functional assay are PFLLR-NH<sub>2</sub> (Table 2, entry 12), SFPLR-NH<sub>2</sub> (entry 14), and NMe-SFLLR-NH<sub>2</sub> (entry 2), in agreement with known topographical requirements (see Introduction); however, receptor recognition (i.e. binding) was only partially affected. It is interesting to note that *N*-Me substitution at position 1 (entry 2) gave a *mixed agonist-antagonist*, whereas proline substitution at position 1 (entry 12) gave a potent agonist. Proline and *N*-methyl substitutions at position 2 are not tolerated, while the N-terminal and P3 through P5 modifications conserve varying degrees of binding affinity. There is a parallelism in receptor binding trends between the ester, *N*-methyl, and proline scans at positions 1 through 5. The α-methyl substitutions

(entries 7–11) are the least tolerated modifications. The difference in functional activity observed between SFPLR-NH<sub>2</sub> (entry 14) and SF-NMeL-LR-NH<sub>2</sub> (entry 4) is rather striking and will be discussed later on.

### Conformational analysis

Computational techniques were used to develop a qualitative impression of the three-dimensional bioactive conformation of TRAP-5. As a starting point, an unrestrained search of the conformational space of TRAP-5 was performed by using a protocol based on the quenched high-temperature molecular-dynamics methodology of Karplus and co-workers.<sup>38,39</sup> This protocol was, in turn, applied to several of the TRAP-5 analogues. Our objective was to develop a picture of the backbone fold and the spatial relationships among the side chains of TRAP-5 that were required for biological activity by correlating the computational results with the biological data.

As a measure of the efficacy of the searches, the distribution of end-to-end distances ( $d_{ij}$ ) and the displacement autocorrelation function of the backbone atoms<sup>39</sup> were computed for each peptide under study. In all cases, the displacement autocorrelation function reached a plateau (Fig. 1a), suggesting that all of the conformational space accessible at 1000 K had been explored. The distribution of end-to-end distances, which ranged from 3.5 to 16 Å in most simulations (Fig. 1b), agrees with what is expected for a flexible pentapeptide. Since the maximum distance between two consecutive residues (e.g. two α-carbons) is ca. 3.6 Å, a fully extended pentamer (β-sheet structure) would have an end-to-end distance of ca. 18 Å. In most cases the distribution of end-to-end distances was uniform in this range, but slightly bimodal distributions, where extended conformations could be distinguished from more collapsed ones, were also observed (Fig. 1b). In any event, the energy histograms always showed a unimodal Gaussian-like pattern (data not shown), as previously reported for peptides.<sup>38</sup>

The results of conformational searches involving α-methyl or *N*-methyl substituted residues were in good agreement with literature data.<sup>34–37</sup> Addition of a methyl group to an amide nitrogen (*N*-Me scan) confined the backbone conformation of the modified residue to four regions of the Ramachandran map (Fig. 2A). The backbone conformation of the preceding residue was, in turn, limited to the upper left-hand quadrant of the map (Fig. 2B). α-Methyl-substituted residues had narrow distributions along the  $\phi = -60^\circ$  and the  $\phi = +60^\circ$  lines in the Ramachandran plane (Fig. 2C). No perturbation of the backbone conformation of neighboring residues was observed.

Among the proline-containing peptides, the case of SFPLR-NH<sub>2</sub> is quite interesting because this peptide is one of the few constrained mimetics with functional activity. As expected, the proline residue has a  $\phi$  dihedral angle centered around  $-60^\circ$  (Fig. 2d). In addition, the prolines, just as the *N*-methyl groups, influence the

residue preceding them (in this case Phe-2), confining the backbone conformation to the same upper left-hand quadrant of the Ramachandran map (Fig. 2B). The differences in the maps of the residue in third position (P3) in SFPLR-NH<sub>2</sub> and SF-NMeL-LR-NH<sub>2</sub> shed some light on the respective biological activity of these two peptides, both of which contain a secondary amide linkage between P2 and P3.

On the basis of these results, a three-dimensional picture of TRAP-5's backbone, in its functional conformation, began to emerge. The main-chain dihedral angles of the Phe residue and the  $\phi$  torsion angle of the third residue (Leu-3) had been circumscribed (Fig. 2B and 2D). The remaining dihedral angle,  $\psi$ , at P3 was still undefined.

To find a basis for selecting the bioactive range, we elected to perform computations on two recently reported<sup>28</sup>  $\beta$ -methylphenylalanine-containing peptides, namely [(3*S*)-3-Me-Phe<sup>2</sup>]TRAP-5 (“*erythro*”) and [(3*R*)-3-Me-Phe<sup>2</sup>]TRAP-5 (“*threo*”). These isomers present an approximately 100-fold difference in functional activity, with the *threo* analogue having virtually the same activity as TRAP-5.<sup>28</sup>

For all searches, the Ramachandran maps of individual residues in the *erythro* peptide and *threo* peptide were essentially identical, indicating that the local backbone folds of the two peptides are very similar (Fig. 3). The features of these maps agree with the results from the other TRAP-5 analogues. The skewed distributions and

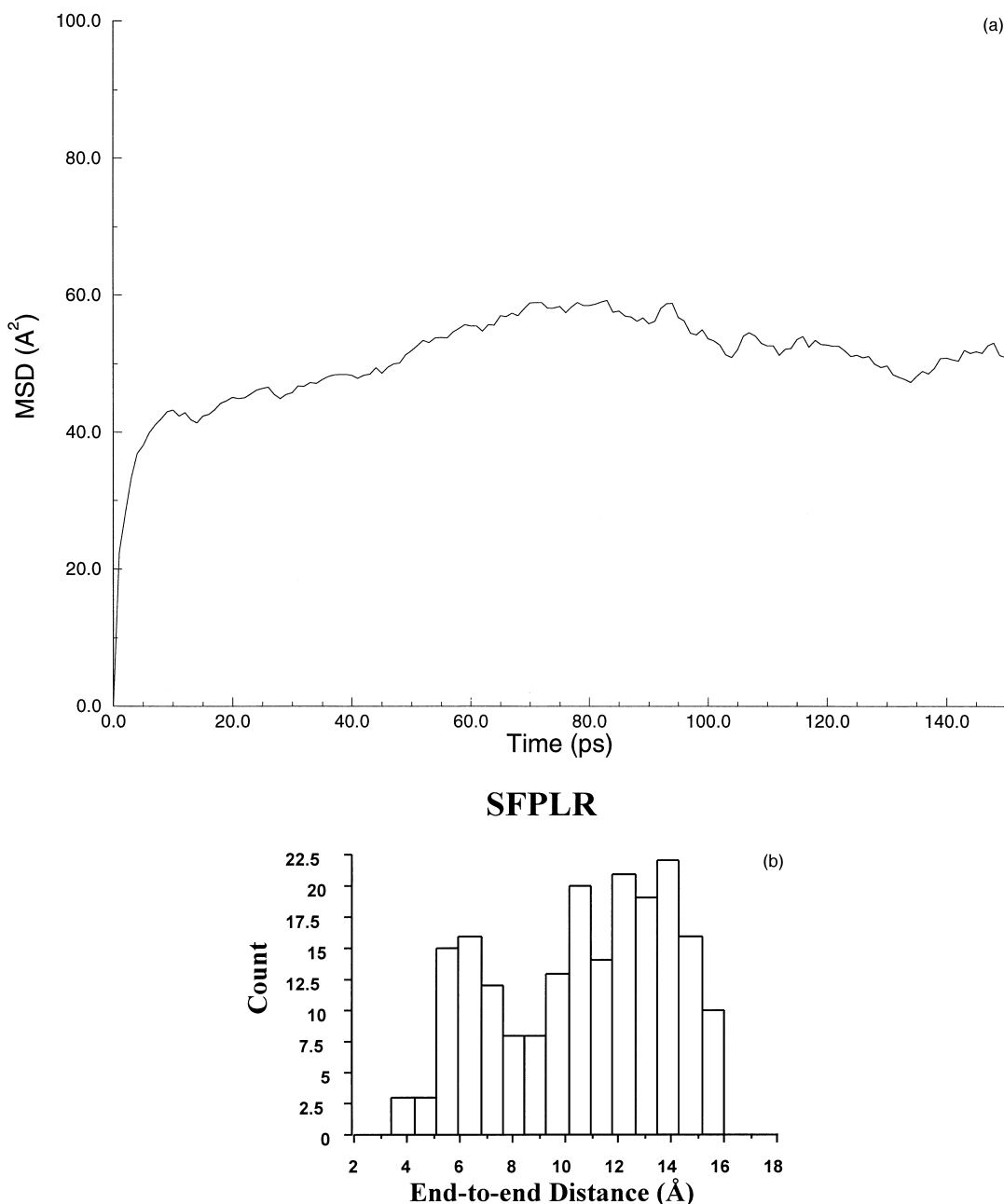


**Figure 1.** Validation of the search protocol. (a) Displacement autocorrelation function obtained for the conformational search of TRAP-5: mean-square atomic displacement (MSD) in time. (b) Distribution of end-to end distances in the case of SFPLR-NH<sub>2</sub>.

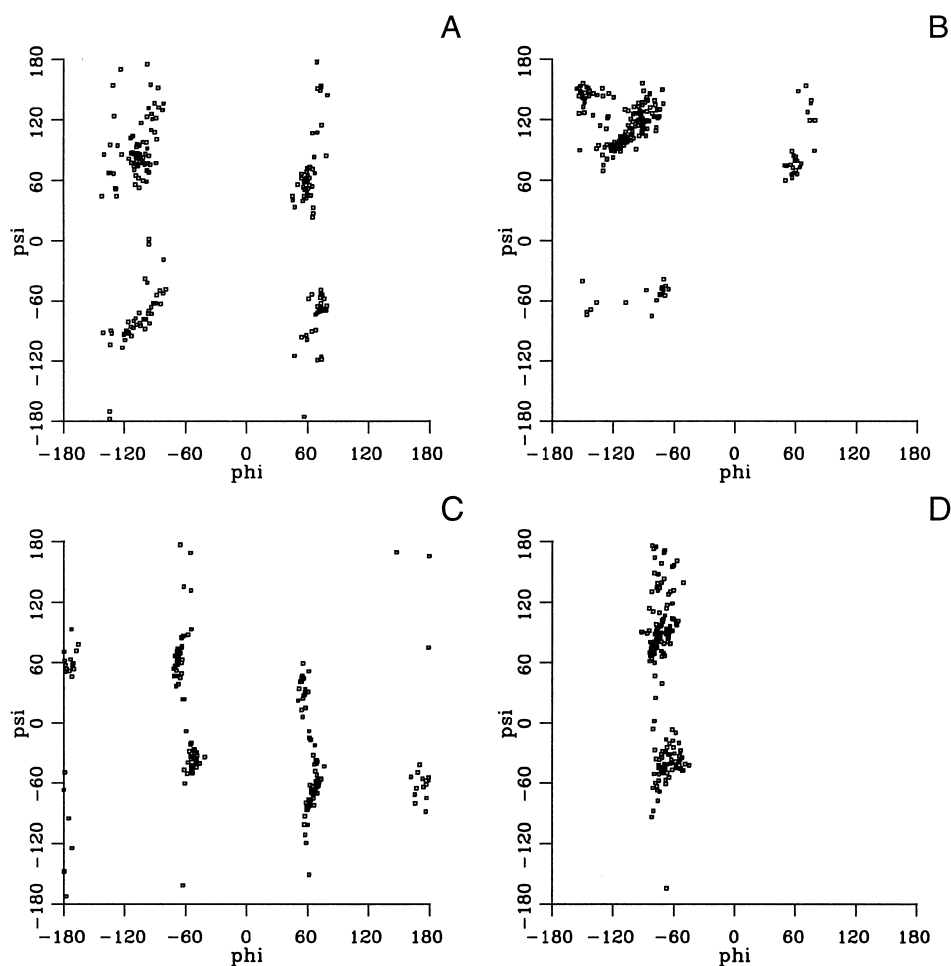


**Figure 2.** Typical phi-psi maps of several locally constrained residues: N-Me-Leu-3 (A) and Phe-2 (B) within SF-(NMeLeu)-LR-NH<sub>2</sub>; Aib-3 (C) within SF-Aib-LR-NH<sub>2</sub>; Pro-3 (D) within SFPLR-NH<sub>2</sub>.

mean values of the end-to-end distances indicate that both peptides preferentially adopt extended conformations (Table 3), but more compact conformations were also observed, as for SFPLR-NH<sub>2</sub> (Fig. 1b). In general, folded/compact structures occurred through formation of a bend at the C-terminus of the peptides (i.e.  $\langle d_{2,5} \rangle$  was less than  $\langle d_{1,4} \rangle$ ).

“Folded” backbone conformations can be identified by the distance ( $d_{i,i+3}$ ) between two C $\alpha$  carbons that are three residues apart: a value of  $d_{i,i+3}$  of less than 7 Å indicates the presence of a bend.<sup>40</sup> Comparison of the means, by using a Student’s *t*-test, indicated that the *erythro* peptide tended to adopt a more compact conformation at its C-terminus than the *threo* peptide: *erythro*  $\langle d_{2,5} \rangle$  less than *threo*  $\langle d_{2,5} \rangle$ . The opposite was true when comparing the N-terminus folds: *threo*  $\langle d_{1,4} \rangle$  less than *erythro*  $\langle d_{1,4} \rangle$ . To gain insight into the structural characteristics of the *threo* and *erythro* peptides, three side-chain-to-side-chain distances were monitored (Table 3). The average distance between the geometric centers of the phenyl ring (at P2) and the guanidinium group (at P5) are statistically similar (95% confidence level) for both diastereomers. The same conclusion was reached for the average distance between the isopropyl group of Leu-4 and the guanidinium

group of Arg-5. On the other hand, the mean distance between the phenyl ring and the isopropyl group of Leu-4 was found to be significantly different (at the 95% confidence level). The *threo* peptide displays a stronger contact between these two side chains than the *erythro* peptide. The  $\chi_1$  dihedral angle distributions at P2 ( $\beta$ -methylphenylalanine) showed that the *threo* peptide adopts mostly *anti* (180°) and *gauche* (+60°) configurations, while the *erythro* peptide principally adopts *gauche*,  $g^+$  (−60°) and  $g^-$  (+60°) orientations. This can serve to explain the greater proximity of the phenyl ring to the isopropyl group of Leu-4 in the *threo* peptide.

To visualize these interactions, the energy-filtered configurations (within 10 kcal/mol of the energy minimum) of the two peptides were superimposed along the backbone atoms of the three central residues:  $\beta$ -MePhe-2, Leu-3, and Leu-4. Hierarchical cluster analysis (average linkage method) was used to classify the configurations of each peptide into distinct families. The results for the *erythro* and *threo* peptides are comparable. In each case, two major families are distinguishable (Figs 4 and 5), and these families adopt similar backbone conformations across enantiomers (Figs 6 and 7). For each peptide, the difference between the two principal families

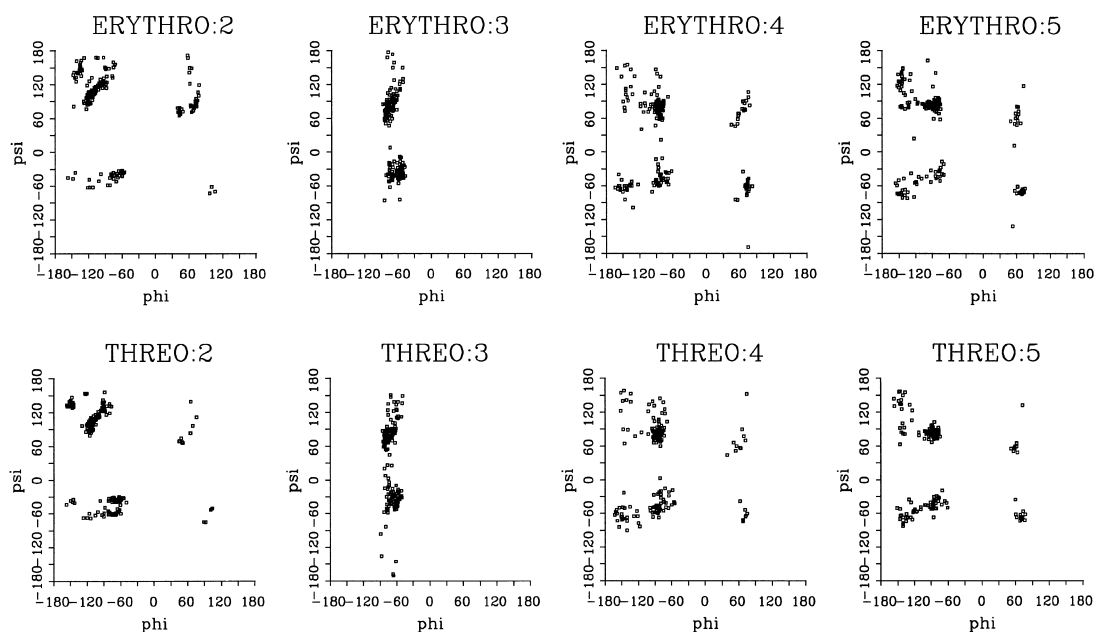


**Figure 3.** Conformational preferences of individual residues in the  $\beta$ -methylphenylalanine-containing peptides. Typical plots of the conformational space sampled during simulation of the “erythro” (top) and “threo” peptides (bottom). Only maps for residues 2–5 are shown (residue number above plot).

**Table 3.** Characteristic distances for the “threo” and “erythro” peptides<sup>a</sup>

Distances	“Erythro” form	“Threo” form
End-to-end distance	11.66 (2.59)	11.78 (3.01)
$C1_{\alpha}-C4_{\alpha}$ : $\langle d_{1,4} \rangle$	8.94 (1.07)	8.62 (1.41)
$C2_{\alpha}-C5_{\alpha}$ : $\langle d_{2,5} \rangle$	7.14 (1.60)	7.64 (1.54)
Side chain-2 $\langle - \rangle$ Side chain-4	8.69 (2.21)	7.74 (2.16)
Side chain-2 $\langle - \rangle$ Side chain-5	8.67 (3.59)	8.75 (3.28)
Side chain-4 $\langle - \rangle$ Side chain-5	9.46 (2.28)	9.37 (2.12)

<sup>a</sup> Average distance in Å with standard deviation in parentheses.

resides mostly in the local backbone conformation of the third residue in the chain (i.e. Leu-3). In the first family, Leu-3 adopts an  $\alpha$ -helical fold, while in the second family, Leu-3 adopts a more extended  $C_7^{eq}$  ( $\phi \approx -80^\circ$ ,  $\psi \approx 80^\circ$ ) conformation, essentially an inverse  $\gamma$ -turn, seven-membered ring structure.<sup>41–43</sup> In both families, the second residue assumes a  $C_5$  ( $\phi \approx -150^\circ$ ,  $\psi = +150^\circ$ ), extended conformation, the fourth residue assumes a  $C_7^{eq}$  conformation, and the last residue (Arg-5) does not appear to favor any particular orientation (i.e. all allowed regions of the Ramachandran map are explored almost equally).

In summary, both isomers were found to exist mainly in extended-type conformations stabilized by at least one backbone hydrogen bond, involving the last three residues in the chain as well as the C-terminal amide group. More compact backbone folds of the C-terminal residues were detected in the case of the virtually inactive erythro peptide,<sup>28</sup> while the bioactive threo peptide<sup>28</sup> showed close hydrophobic contacts between the P2 and P4 side chains. The organization of the core residues Phe-2, Leu-3, and Leu-4 was mostly determined by the local conformation of Leu-3. The N-terminal serine was not a structural determinant for the core residues and

the side chain of Arg-5 was very flexible, without preferential orientation with respect to the rest of the chain (Figs 4 and 5).

Presently, in terms of favored bioactive conformations for TRAP-5, the data highlight the importance of the carbonyl groups as hydrogen-bond acceptors, whether they are involved in an intermolecular (ligand-receptor) or an intramolecular sense. Independently of how folded or extended TRAP-5 may be, the spatial placement of the Phe-2 and Leu-4 side chains, which is governed by the local conformation of Leu-3, appears to be a key factor for determining biological activity.

### Spectroscopic studies

To test the validity of the above model and to discern the local conformation at Leu-3, physical experiments were conducted. Because short linear peptides are extremely flexible in aqueous solution, the conformational properties were studied in the presence of 2,2,2-trifluoroethanol (TFE). It was hoped that this more acidic, polar solvent would stabilize transiently ordered structures (e.g. a turn at Leu-3) by competing less effectively with intramolecular hydrogen bonding.

Circular dichroism (CD) is a powerful tool for monitoring conformational changes and estimating secondary structures in peptides and proteins. The CD absorption of TRAP-5 showed that, on titration with TFE, the peptide was capable of populating nonrandom-coil conformations (Fig. 8A), as particularly reflected by an intense positive absorption band around 190 nm. No effort was made to interpret the spectrum further in terms of specific secondary structure, but it was important to establish that under adequate conditions TRAP-5 could exist in disordered and

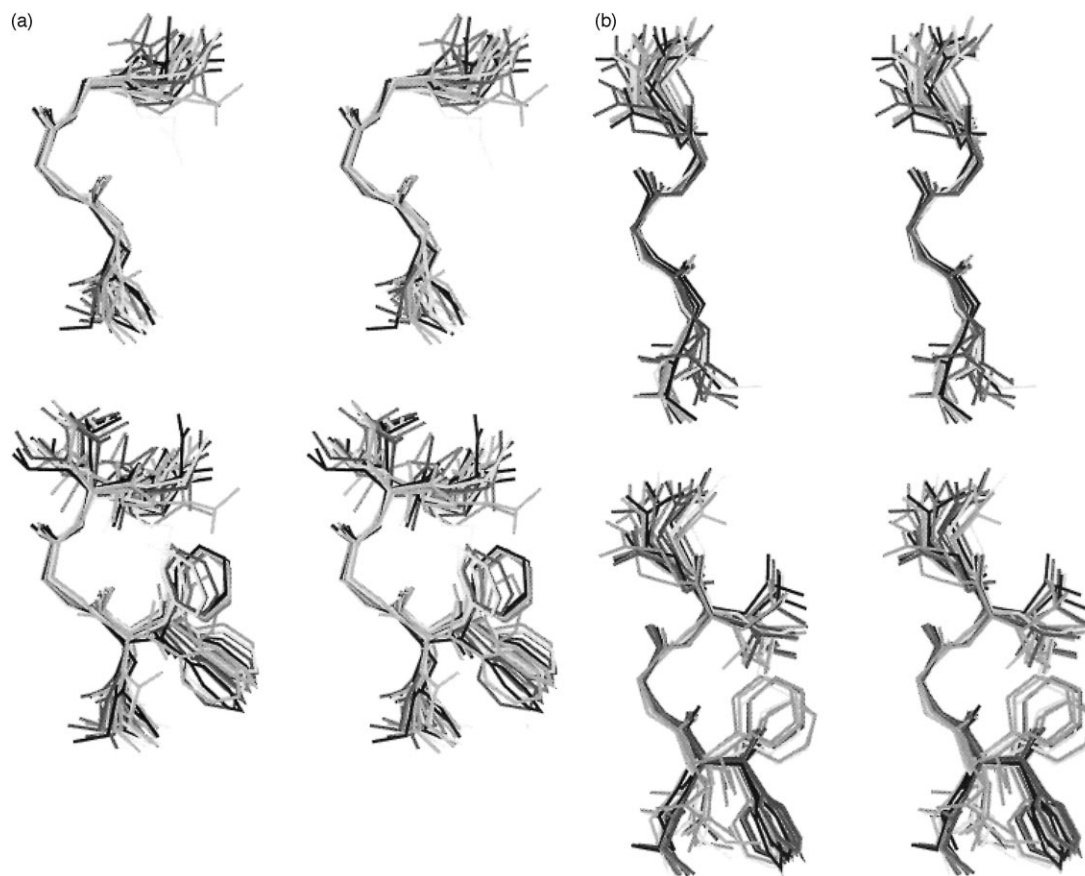


**Figure 4.** Stereoviews of the most populated backbone conformations of the “*threo*” peptide: (A) second family: backbone-only representation (top), backbone plus side chains of residues at P2 and P4 (bottom); (B) fifth family: corresponding views.

ordered (not necessarily with a bend in the sequence) conformations, as the computer simulations suggested.

To unveil the hydrogen-bonding patterns responsible for the stability of such conformations, all ester and reduced-amide derivatives were examined under similar conditions (Fig. 8B and C). Substantial changes in the CD absorption for TRAP-5 occurred when either central amide bond,  $\Psi_{2,3}$  or  $\Psi_{3,4}$ , was replaced with an ester or reduced-amide linkage. Besides changes at shorter wavelength, significant variations in the sign and intensity of the Cotton effect at longer wavelengths (i.e. at ca. 230 nm) were observed. Such patterns have been shown to reflect the handedness of the turn or helical structure in a peptide.<sup>44,45</sup> Conversely, replacement of the first or last amide bond of TRAP-5,  $\Psi_{1,2}$  or  $\Psi_{4,5}$ , led to much less dramatic changes in the CD absorption spectra of those peptides. These data confirm the importance of the central residue, Leu-3, for the three-dimensional organization and biological activity of the agonist peptides.

Rigidified peptides **1–5** were synthesized in an attempt to probe the role of the P3 residue in TRAP-5’s structure (Table 4). These peptides, which contain cyclic amino acids with 1,2- and 1,3-disubstituted rings (**1–5**), were not very biologically active as agonists, or antagonists. Although **1A**, one of the four peptide diastereomers with the 1,3-substituted cyclohexyl ring

(**1A/B**, **2A/B**), showed some affinity for PAR-1, it did not activate the receptor nor act as an antagonist. These subunits introduce one or two additional carbons into the backbone chain relative to the TRAP-5, which probably separates the P2 and P4 side chains at too great a distance to permit agonist action.

Compounds **1A**, **2** and **3** (Table 4) and TRAP-5 were studied by <sup>1</sup>H NMR in 50% TFE at 278 K. As indicated by the <sup>3</sup>J<sub>HN-H $\alpha$</sub>  coupling constants of ca. 7 Hz and the amide temperature coefficients in the range of 6 and 8 ppb/K, all of the peptides showed substantial conformational averaging. In **1A** and TRAP-5 there was a nuclear Overhauser effect (NOE) contact between the side chains of residues 2 and 4. This result is interesting because, despite the presence of two extra carbons in the backbone, **1A** possesses sufficient conformational flexibility to establish the native NOE contact seen in TRAP-5 (which is absent with the 1,2-disubstituted case). However, this capacity of **1A** was not sufficient to elicit the native biological response.

To gauge the significance of the contact between Phe-2 and Leu-4, we can consider TRAP-5 analogues with the native leucine at position 4 mutated to valine, alanine, or glycine. The platelet activation EC<sub>50</sub> values for SFLVR-NH<sub>2</sub> (L4V), SFLAR-NH<sub>2</sub> (L4A), and SFLGR-NH<sub>2</sub> (L4G) were determined to be 130, 3.4, and 120  $\mu$ M, respectively, compared with 0.49  $\mu$ M for TRAP-5, while

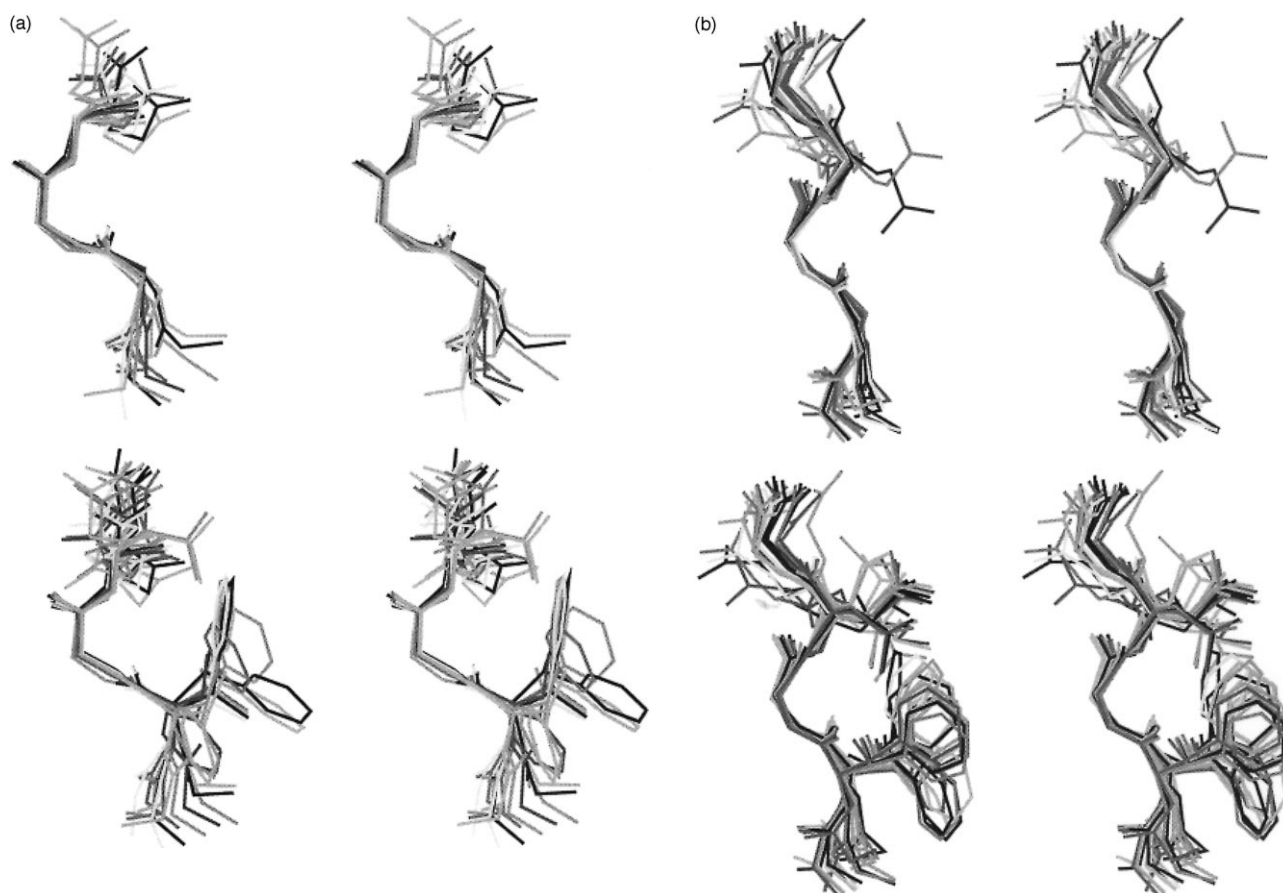


**Figure 5.** Stereoviews of the two most populated backbone conformations of the “*erthro*” peptide: (A) third family: backbone-only representation (top), backbone plus side chains of residues at P2 and P4 (bottom); (B) fifth family: corresponding views.

the receptor binding  $IC_{50}$  values were 9.3, 1.8, and  $7.4 \mu\text{M}$ , respectively, compared with  $1.5 \mu\text{M}$  for TRAP-5. The functional activity was attenuated for all three P4 mutants, to the extent of 25-fold, 7-fold, and 25-fold, respectively. However, the receptor binding was attenuated for just two of the P4 mutants: 6-fold for L4V and 5-fold for L4G. The loss in functional activity agrees with results reported by others,<sup>25,26</sup> who found that substitution with other aliphatic residues usually gives diminished platelet agonist activity, although norleucine (Nle) was slightly better than leucine. It was also reported that aromatic residues, such as F, W and Y, are well tolerated at position 4, lending support to the idea of hydrophobic interaction between positions 2 and 4.<sup>26</sup>

Overall, the peptide series that we studied from a conformational aspect point to a pivotal role for P3 in controlling the backbone conformation, the orientation of critical side chains, and the nature of the biological response.

### Discussion

The biological activity of agonist peptide ligands interacting with the thrombin receptor (PAR-1) results from

binding and signal transduction events, whereas antagonist ligands would bind effectively but not transduce a signal into the cell. For a ligand with many possible conformations in solution, it is likely that an “induced-fit” model of ligand-receptor interaction, in which there is mutual conformational adjustment of both the ligand and the receptor macromolecule, is operative, rather than a “lock-and-key” model.<sup>46,47</sup> In the induced-fit model, the initial recognition event is followed by a cascade of transformations where the ligand and receptor cooperatively evolve to produce a biologically relevant (agonist or antagonist) three-dimensional complex. The following discussion pertains to structure-function analysis of the topographical (specific chemical groups) and geometrical (specific spatial arrangements) features that characterize our TRAP-5 analogues.

### Polarity, orientation, and steric bulk at the N-terminus

Recently, Bernatowitz et al.<sup>48</sup> reported the existence of an active TRAP-5 mimic with an uncharged N-terminus: Ac- $\beta$ -Ala-FLLR-NH<sub>2</sub>. This is an unusual result since a positively charged N-terminus has generally been presented as a key feature for agonist activity (see Introduction). In fact, for this analogue the importance of the additional methylene group (introduced within

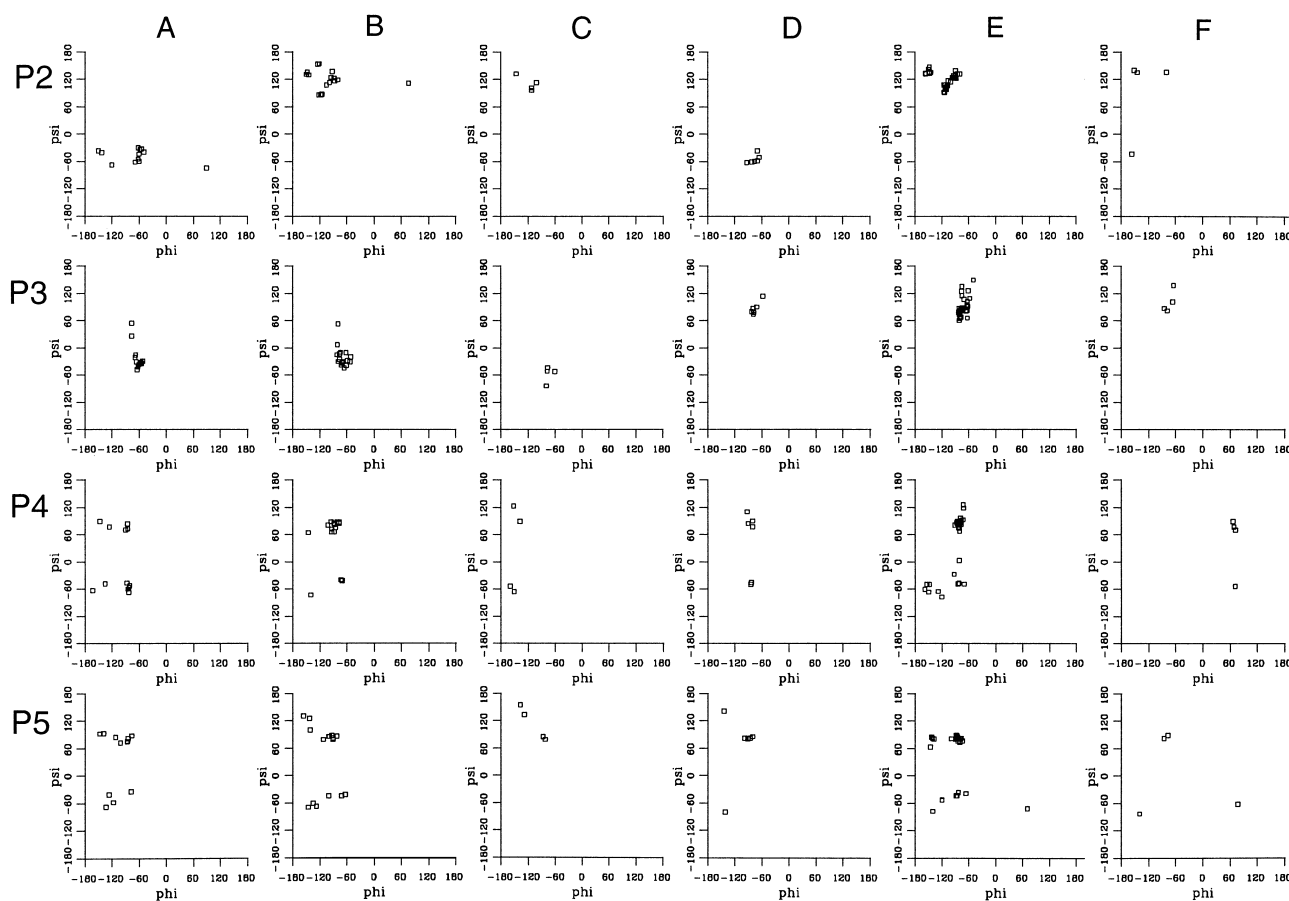


**Figure 6.** Ramachandran plots of individual residues in the “*threo*” peptide (residues P2–P5 only), grouped by family clusters (columns A–F). Most populated clusters appear in the second family (column B) and fifth family (column E). Low population families are not presented.

the  $\beta$ -alanine residue) should not be underestimated since acetylation of the N-terminus of standard agonist peptide sequences has led to a complete loss of activity.<sup>14,22,25,49</sup> This suggests that Ac- $\beta$ -alanine analogues are forming new interactions with the receptor that are capable of compensating for the absence of the original charged N-terminus, probably via the N-acetyl group. This may explain why the shorter Ac-Ala peptide is inactive, and why the de-acetylated version,  $\beta$ -Ala-FLLR-NH<sub>2</sub>, is inactive.<sup>49</sup> However, it is possible to retrieve biological activity in the native pocket with just a polar N-terminus according to our results with  $\Psi(\text{HO})\text{S-FLLR-NH}_2$  and  $\Psi(\text{HO})\text{A-FLLR-NH}_2$  (Table 1, entries 8 and 7). In this case, because of their similarity in size, the N-termini are probably interacting within the native pocket, rather than farther away. For this to occur, it appears that there must be strict limitations on steric bulk (see Introduction) and strict requirements on polarity and orientation. With respect to alteration of the residue at the N-terminus, it is worth recounting that proline substitution at position 1 (Table 2, entry 12) resulted in a potent agonist, and *N*-Me substitution at position 1 (Table 2, entry 2) resulted in moderated agonist activity along with an antagonist component.

While the effect of steric bulk has already been described in the literature, the orientational preferences at position 1 start to become apparent with the lack of

activity of  $\alpha$ -methyl-substituted residues such as  $\alpha$ -MeS-FLLR-NH<sub>2</sub> (Table 2) and Aib-FLLR-NH<sub>2</sub> (data not shown).<sup>25</sup> The steric bulk introduced by the methyl substitution could be responsible for the ineffectiveness of these analogues, but for S- $\Psi(\text{COO})\text{-FLLR-NH}_2$  (Table 1) the change in conformational preferences, which is apparent in CD studies (Fig. 8B), might support a stereospecific requirement rather than a regio-specific one.

### Backbone requirements for recognition and activity

Substitutions involving peptide bond modifications had dramatic structural (and biological) effects. From a conformational point of view, CD studies showed the existence of a certain parallelism between ester bond replacements and their corresponding reduced-amide bond homologues. That is, a modification at a given amide bond produced similar effects on replacement of either the amide nitrogen or the carbonyl oxygen (Fig. 8B and C). In the biological studies, this *correspondence* disappeared, as only one TRAP-5 analogue, SF- $\Psi(\text{COO})\text{-LLR-NH}_2$ , conserved functional activity. The peptide bond replacements seemed to impact on different stages of the recognition process. Designating the NH group between residues *i* and *j* as NH<sub>*ij*</sub>, the data in Table 1 suggest that NH<sub>12</sub> and NH<sub>34</sub> are needed at the inception of ligand-receptor recognition, that NH<sub>45</sub> is

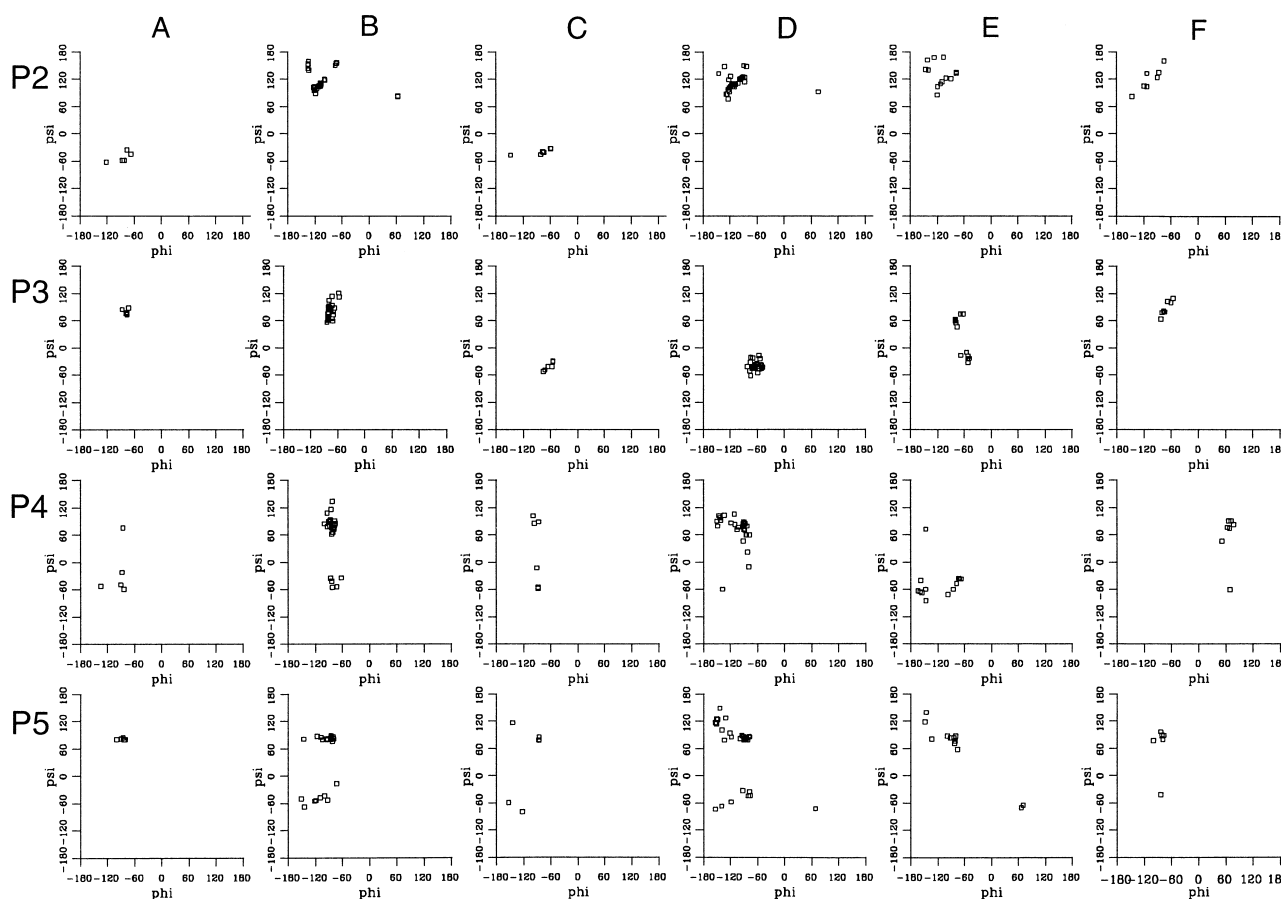


**Figure 7.** Ramachandran plots of individual residues in the “erythro” peptide (residues P2–P5 only), grouped by family clusters (columns A–F). Most populated clusters appear in the third family (column C) and fifth family (column E). Low population families are not presented.

only involved at the activation stage, and that NH<sub>23</sub> is not involved at all in ligand-receptor interaction. The case of NH<sub>34</sub> is not clear since its binding constant adopts an intermediate value which has to be appreciated in combination with those of SFL-NMeL-R-NH<sub>2</sub> and SFPLR-NH<sub>2</sub> (Table 2). This peptide bond could have partial involvement both at the recognition and activation stages, since the lack of biological activity here could arise from conformational rather than topographical (i.e. absence of an amide hydrogen) sources. On the other hand, carbonyl mutation at any position prevented recognition of the peptide by the receptor, which is not uncommon with reduced-amide scans.<sup>50–53</sup> Although these reduced-amide homologues may be expected to possess greater conformational flexibility, the loss in recognition/activity could be attributed to an unfavorably biased conformational distribution. On protonation, the presence of a strong NH<sup>+</sup> hydrogen bond with a neighboring carbonyl (ten-membered ring) would stabilize a  $\beta$ -turn-like conformation,<sup>52,53</sup> which may preclude formation of the putative bioactive conformation, i.e. one with a more extended backbone.

Six out of eight NH and C=O groups are required at the inception of recognition. This could reflect the fact that one or more of the NH/carbonyl groups needs to interact directly with the receptor to stabilize the bound conformation of TRAP-5 (intermolecular role).

Alternatively, one or more of these groups could be used by the peptide to “lock” itself into a conformation that would then bind to the receptor (intramolecular role). Finally, a combination of intermolecular and intramolecular components may also pertain. Several pieces of information weaken the intramolecular hydrogen bonding interpretation. First, given the reciprocity of hydrogen bond donors and acceptors, the fact that all of the amine-for-amide substitutions resulted in a loss receptor binding, whereas four of the five ester-for-amide substitutions did not (Table 1, entries 3, 5, 6, and 7), suggests that only the NH of the Phe residue and one of the carbonyls are candidates for intramolecular hydrogen bonding. However, this view is not supported by the Phe amide <sup>1</sup>H NMR temperature coefficient. Secondly, the *loss* of the conformational/biological *correspondence* between the ester and reduced-amide peptides indicates that, although the peptides populate similar conformational ensembles, their capacity to be recognized is different. These observations serve to distinguish the recognition-stage conformation of the ligand from its receptor-bound conformation. Consequently, with the large number of backbone interactions that are necessary, an extended conformation of the peptide appears most probable at an initial stage of interaction with the receptor. Extended conformations are not uncommon for peptide ligands<sup>54,55</sup> and, more specifically, Siligardi and Drake<sup>56</sup> have

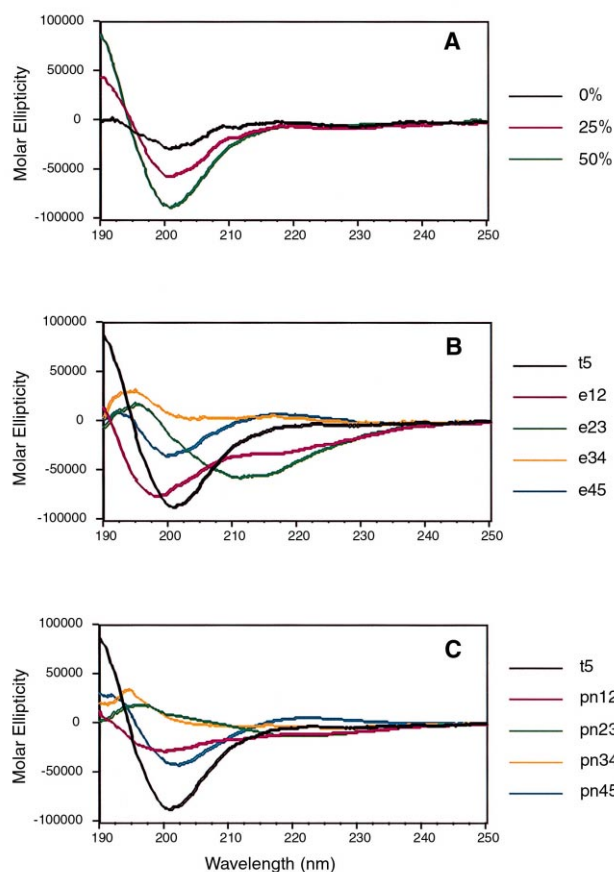


**Figure 8.** CD spectra of TRAP-5 (t5) and peptide-bond surrogate  $\Psi(\text{CH}_2\text{NH})$  and  $\Psi(\text{COO})$  analogues: (A) CD of TRAP-5 in increasing amounts of TFE; (B) comparison of TRAP-5 and  $\Psi(\text{COO})$  analogues in 50% TFE; (C) comparison of TRAP-5 and  $\Psi(\text{CH}_2\text{NH})$  analogues in 50% TFE. The parameters  $e_{ij}$  and  $pn_{ij}$  designate the pentapeptide for which the amide bond between residues  $i$  and  $j$  was replaced, respectively, by an ester or a secondary amine.

underscored the importance of the  $P_{II}$  conformation in molecular recognition.

In summary, an extended conformation appears to be a probable structure for agonist peptide binding to PAR-1 (i.e. receptor recognition), although intermolecular hydrogen bonding between the peptide backbone and receptor may not be uniform throughout the sequence. Intramolecular hydrogen bonding may also give rise to a locally folded conformation that plays a role in ligand-induced signal transduction (i.e. receptor activation).

### Position 3 as a key structural element

Position 3 (P3) appears to play a special role in TRAP-5. A wide variety of side chains can be tolerated in this position and we determined herein that the amide nitrogen can be substituted by an oxygen, as in SF- $\Psi(\text{COO})\text{-LLR-NH}_2$ , without loss of bioactivity. On the other hand, this peptide bond is sensitive to conformational changes. For example, while SFPLR- $\text{NH}_2$  is active, SF-NMeL- $\text{LR-NH}_2$  is not. Our computational studies point out the slightly different conformational preferences of P3 in these two peptides (cf. Figs 2D and

**Table 4.** Biological data for some P3-constrained analogues of TRAP-5

Compound	Residue at P3 SF-X-LR-NH <sub>2</sub>	Platelet aggregation <sup>a</sup> EC <sub>50</sub> (μM)	Receptor binding <sup>b</sup> IC <sub>50</sub> (μM)
<b>1A</b> <sup>c</sup>		> 50 (5%)	8
<b>1B</b> <sup>c</sup>		> 50 (7%)	> 100
<b>2A</b> <sup>c</sup>		> 50 (6%)	
<b>2B</b> <sup>c</sup>		> 50 (6%)	
<b>3</b> <sup>d</sup>		> 50 (5%)	66
<b>4</b> <sup>d</sup>		> 50 (9%)	> 100
<b>5A</b> <sup>c</sup>		> 50 (40%)	96
<b>5B</b> <sup>c</sup>		> 50 (39%)	40

<sup>a</sup> See Table 1.

<sup>b</sup> See Table 1.

<sup>c</sup> Two diastereomers, **A** and **B**, were isolated and evaluated independently.

<sup>d</sup> Mixture of diastereomers.

2A). Similarly, SF- $\alpha\text{MeL-LR-NH}_2$  is also inactive; however, in this case steric bulk, as well as conformational constraint, could be a problem. Computational, <sup>1</sup>H NMR, and P4 mutation data (*vide supra*) suggest a possible cause for this conformational sensitivity: the presence of hydrophobic contact between the Phe-2 and Leu-4 side chains. This interaction is reminiscent of a hydrophobic staple motif, which applies to these same residues in some instances.<sup>57</sup> This structural motif, which has an important role in the stabilization of peptide helices, is based on hydrophobic contact between the  $i$  and  $i+4$  residues in the helix, and the distance between such residues is comparable to that identified in our modeling studies. However, such hydrophobic contact is not a sufficient condition for inducing a biological response, as indicated by the 1,3-disubstituted cyclohexyl analogue, **1A**, which should be capable of the necessary contacts but is devoid of agonist activity.

Another notable trait of P3 is the intolerance for a rigid spacer, such as a 3-aminocyclohexyl-1-carboxylic acid, which introduces two more carbon atoms into the backbone chain (Table 4). Also, the 1,2-disubstituted analogues, which introduce only one such carbon, are inactive (Table 4). In **1–5** there may be a likelihood of reorientation of the peptide backbone, because of the conformational constraint at position 3, to generate a different type of peptide chain.

In any event, we suggest that the conformational sensitivity at P3 is linked with hydrophobic contact between Phe-2 and Leu-4. The P3 region might act as a conformational switch to enable or disable the formation of either the agonist complex with PAR-1 by orchestrating

an interaction between Phe-2 and Leu-4, and possibly involving Arg-5.

### Conclusion

In addition to the well-known structural features of PAR-1 agonist peptides, this work has presented an analysis of the topographical requirements of TRAPs in conjunction with PAR-1 binding and functional activity. The absolute requirement of a positive N-terminal charge of  $\text{NH}_3^+$  to exhibit strong agonist activity was contradicted, consistent with another recent result in the literature,<sup>48</sup> as a hydroxyl group can suffice. The amide nitrogen between residues 1 and 2 was identified as a key determinant for receptor recognition. Also, carbonyl groups along the backbone appear to be involved in hydrogen bonding with the receptor. We elucidated conformational and local geometrical features, leading to our proposal that an extended form of the agonist peptide is required for receptor recognition (i.e. PAR-1 binding). This conformational viewpoint generally agrees with that proposed by Shimamoto et al.<sup>28</sup>

During the course of our studies, Matsoukas et al.<sup>58</sup> published a report on the conformation of SFLLR-NH<sub>2</sub> in dimethylsulfoxide (polar, aprotic conditions), in which they proposed a curved (“cyclic”) backbone for the active form of TRAP-5 because of weak NOE contacts between the Arg-5 side chain and the Ser-1 and Phe-2 residues. We found no side-chain contacts of this kind under our experimental conditions (polar, protic), nor in our computational searches. With SFPGR-NH<sub>2</sub>, where the PG sequence should encourage a  $\beta$ -turn geometry, we did observe an NOE between Phe-2 and Arg-5; however, this analogue failed to bind to PAR-1 ( $\text{IC}_{50} > 100 \mu\text{M}$ ).

Matsoukas et al. gleaned further support for a “cyclic” backbone for agonist peptides from macrocyclic analogues of SFLLR-NH<sub>2</sub>,<sup>59</sup> since macrocyclic peptides tend to adopt folded conformations, such as  $\beta$ - and/or  $\gamma$ -turns, fixed by intramolecular hydrogen bonding (although this influence can vary with ring size). Since a 19-membered-ring macrocyclic SFLLR analogue linked from the P1 side chain to the C-terminus was nearly equipotent with SFLLR-NH<sub>2</sub> in inducing contractions of gastric smooth muscle,<sup>60,61</sup> they proposed that the agonist motif approaches the receptor in a “cyclic” conformation with spatial proximity of the Phe-2 and Arg-5 side chains. However, one should keep in mind that a macrocyclic peptide can still experience an induced conformation on complexation with a receptor, or present a linear (extended) motif if the macrocycle is sufficiently large and flexible.<sup>62</sup>

An important aspect of our conformational studies of the SFLLR motif is the indication of hydrophobic contact between the side chains of the second and fourth residues (P2-P4 interaction), which differs from the P2-P5 side chain interaction proposed by Matsoukas et al.<sup>58</sup> The spatial arrangement of the P2 and P4 side chains might be responsible for determining the agonist

or antagonist nature of the ligand-receptor complex and thus be useful in the design of novel agonist or antagonist molecules for the thrombin receptor (PAR-1).

### Experimental

**Materials.** Synthesis solvents were HPLC grade and obtained from Fisher or VWR Scientific. Commercially available reagents, unless otherwise noted, were used without further purification. Rink-amide resin was purchased from Advanced ChemTech with a measured loading of 0.46–0.67 mmol/g; 4-methylbenzhydrylamine resin (MBHA) was purchased from Bachem Bioscience with a loading of 0.66 mmol/g. Fmoc- and Boc-protected amino acids were purchased from Novabiochem and Bachem Bioscience. DIC, HOBT, BOP-Cl, DMAP, Fmoc-Cl, piperidine, TFA, L-2-hydroxy-isocaproic acid, L-3-phenyllactic acid, and calcium L-glycerate were purchased from Aldrich Chemical Co. L-Argininic acid and  $\alpha$ -methyl-D,L-leucine were purchased from Sigma, *cis*-3-aminocyclohexanecarboxylic acid was purchased from TCI, and L- $\alpha$ -methylphenylalanine was purchased from Novabiochem. (*S*)-2-Amino-2-methyl-3-hydroxypropanoic acid, *cis*- and *trans*-2-amino-1-cyclohexanecarboxylic acids, and *cis*-2-amino-1-cyclopentanecarboxylic acid were purchased from Acros. Purchased amino acids that required Fmoc protection were acylated by using Fmoc-Cl and sodium carbonate following the procedure of Carpino and Han.<sup>63</sup> L- $\alpha$ -Methylarginine was prepared from *rac*-2-methylornithine (Aldrich) according to the method of Roeske et al.<sup>64</sup> The Boc-protected  $\alpha$ -amino aldehydes were prepared from the corresponding alcohols (Bachem Bioscience) via sulfur trioxide/pyridine oxidation.<sup>65</sup> Hour-glass bubbler reactors were purchased from Peptides International.

**Methods.** <sup>1</sup>H NMR spectra for analytical purposes were recorded on a Bruker AC-300 (300 MHz) or a Bruker AM-400 (400 MHz) spectrometer with D<sub>2</sub>O as solvent, locked on the solvent, unless otherwise noted (s = singlet, d = doublet, t = triplet, m = multiplet, dd = doublet of doublets, br = broadened); Me<sub>4</sub>Si was used as internal standard for nonaqueous solutions. Standard fast-atom bombardment (FAB) mass spectra were obtained on a VG 7070E high-resolution mass spectrometer and electrospray (ES) mass spectra were obtained on a VG Trio 2000 mass spectrometer. Accurate mass measurements (HRMS) were obtained by using a VG ZAB 2-SE spectrometer in the FAB mode. Peptide purification was accomplished by semi-preparative HPLC on a Waters 600E instrument (Waters 486 detector) with a reverse-phase column [Waters Bondapak C18, 40×100 mm (three in series, 125 Å, 15–20  $\mu\text{m}$ ), Bondapak C18, 3.9×300 mm (100 Å, 10  $\mu\text{m}$ ), or Delta-Pak C18, 8×100 mm (100 Å, 15  $\mu\text{m}$ )], eluting with a mixture of 0.16% TFA in acetonitrile and 0.20% TFA/water in isocratic or gradient modes.

**Synthesis of conventional peptides.** Conventional peptides involving native amino acids and *N*-methyl peptides (Tables 1 and 2) were synthesized by stepwise

solid-phase synthesis employing Applied Biosystems Model 431A or Model 430A peptide synthesizers with Boc/benzyl chemistry on MBHA or PAM (phenylacetamidomethyl) resins according to the manufacturer's instructions. The assembled peptide resins were deprotected and the peptides were released from the resin by using standard liquid HF procedures to afford the crude peptides. Each peptide was purified to homogeneity by reverse-phase HPLC on a Waters Delta-Pak C18 column with gradient elution using acetonitrile in water containing 0.1% trifluoroacetic acid. Purified peptides were reanalyzed by reverse-phase HPLC on a Vydac C18 analytical column to ensure purity (>95%). FABMS was used to confirm the structure of each peptide.

#### General procedure for the preparation of depsipeptides.

The esters were prepared via solid-phase synthesis employing the Rink-amide resin and an Fmoc protocol in the customary fashion.<sup>66–68</sup> Piperidine in DMF (20% v/v, 10 mL) was used to cleave the Fmoc protection from the growing peptide (0.1 mmol), and couplings between Fmoc protected amino acids (0.3 mmol) or the  $\alpha$ -hydroxy acid (0.3 mmol) and the peptide on resin were performed with DIC (0.3 mmol) and HOBT (0.3 mmol) in DMF. BOP-Cl (0.3 mmol) and DMAP<sup>69</sup> (0.6 mmol) in CH<sub>2</sub>Cl<sub>2</sub> (10 mL) was used to couple the resin-bound hydroxy peptide (0.1 mmol) to the next Fmoc-protected amino acid (0.3 mmol) to form the ester bond. After final Fmoc deprotection, cleavage from the resin and concomitant arginine side-chain PMC deprotection was accomplished with 99% TFA at 23°C to afford the desired product as the trifluoroacetate salt. These materials were purified by reverse-phase semi-preparative HPLC, followed by lyophilization to give the depsipeptides as white solids.

#### Examples A

**A. Synthesis of H<sub>2</sub>N-Ser-Phe-Leu- $\Psi$ (COO)-Leu-Arg-NH<sub>2</sub>.** Rink-amide resin (4.98 g, 0.46 mmol/g, 2.3 mmol) was placed in an hour-glass bubbler reactor, washed twice with DMF (30 mL) and agitated (nitrogen) with 20% piperidine in DMF (30 mL) for 1 h at 23°C and the solution drawn off. The resin was washed with fresh DMF (4 $\times$ ), CH<sub>2</sub>Cl<sub>2</sub> (3 $\times$ ), and DMF (3 $\times$ ). Fmoc-Arg-(PMC)-OH (5.36 g, 7 mmol), HOBT (1.2 g, 7.8 mmol) and DIC (0.88 g, 7 mmol) were added and slurried with DMF (30 mL) and the mixture was agitated for 16 h. The solution was drawn off and the resin was washed with DMF (4 $\times$ ), CH<sub>2</sub>Cl<sub>2</sub> (4 $\times$ ) and dried in vacuo at 25°C for 24 h. The Fmoc arginine-loaded resin (0.75 g, 0.33 mmol) was deprotected with 20% piperidine in DMF (15 mL) and washed as above, then combined with L-2-hydroxyisocaproic acid (132 mg, 1 mmol), HOBT (150 mg, 1 mmol), and DIC (126 mg, 1 mmol) in DMF (10 mL) and agitated for 3 h. After the solution was removed, the resin was washed with DMF (4 $\times$ ) and dry (4A sieves) CH<sub>2</sub>Cl<sub>2</sub> (4 $\times$ ) and then combined with Fmoc-Leu-OH (370 mg, 1.05 mmol) and DMAP (0.26 g, 2.1 mmol) in CH<sub>2</sub>Cl<sub>2</sub> (10 mL) and agitated (with argon) as BOP-Cl (0.26 g, 1 mmol) was added to the mixture. Agitation was continued for 7 h at 23°C with periodic addition of dry CH<sub>2</sub>Cl<sub>2</sub> to replace evaporated solvent. Solution was drained off and the resin was washed with

CH<sub>2</sub>Cl<sub>2</sub> (3 $\times$ ), DMF (3 $\times$ ), and CH<sub>2</sub>Cl<sub>2</sub> (3 $\times$ ) and dried under an argon stream; this peptido-resin was stored at 0°C. Fmoc deprotection was repeated as above and the resin was combined with Fmoc-Phe-OH (387 mg, 1 mmol), HOBT (150 mg, 1 mmol), and DIC (126 mg, 1 mmol) in DMF (10 mL) and agitated for 2 h. The solution was drained off and the resin was washed with DMF (5 $\times$ ). Fmoc deprotection was repeated and the functionalized resin was combined with Fmoc-Ser(*O*-*t*-Bu)-OH (0.38 g, 1 mmol), HOBT (150 mg, 1 mmol), and DIC (126 mg, 1 mmol) in DMF (15 mL) and agitated for 4 h. After washing, the resin was carefully deprotected (to avoid reaction of the terminal amine with the ester) with 20% piperidine in DMF (15 mL) at 23°C for 12 min and washed with DMF (3 $\times$ ) and dry CH<sub>2</sub>Cl<sub>2</sub> (3 $\times$ ), then dried under a nitrogen stream. Peptide cleavage was accomplished by agitation of the resin with 99% TFA (20 mL) at 23°C for 2 h. The red solution was drained and evaporated in vacuo to an oil, which was triturated with ethyl ether (2 $\times$ , 25 mL) to a white solid (140 mg). The peptide was purified by reverse-phase HPLC by using the Waters Bondapak C18 column (40 $\times$ 100 mm) and 0.16% TFA in acetonitrile:0.20% TFA in water (30:70) as an eluent. The solution was evaporated in vacuo and the solid was redissolved in water. This aqueous solution was frozen and lyophilized to afford a white amorphous solid (42 mg). FAB-MS  $m/z$  635.5 (MH<sup>+</sup>); <sup>1</sup>H NMR (400 MHz, CD<sub>3</sub>OD)  $\delta$  0.88–1.00 (2 pairs of d, 12H), 1.58–1.96 (m, 10H), 2.89 (dd,  $J$ =10.3, 12.8 Hz, 1H), 3.15–3.40 (m, 3H), 3.78–3.97 (m, 3H), 4.36–4.53 (m, 2H), 4.74 (dd,  $J$ =4.0, 8.0 Hz, 1H), 5.05 (dd,  $J$ =4.0, 9.5 Hz, 1H), 7.18–7.35 (m, 5H, arom.), 8.10 (d, exch. H), 8.40 (d, exch. H). Anal. (C<sub>30</sub>H<sub>50</sub>N<sub>8</sub>O<sub>7</sub>·3.0 CF<sub>3</sub>CO<sub>2</sub>H): C, H, N.

**B. Other depsipeptides.** In the same manner, the following depsipeptides (oxygen isosteres) were prepared. (1)  $\Psi$ (HO)Ser-Phe-Leu-Leu-Arg-NH<sub>2</sub>: ES-MS  $m/z$  635.4 (MH<sup>+</sup>), <sup>1</sup>H NMR (400 MHz, DMSO-*d*<sub>6</sub>); (2)  $\Psi$ (HO)Ala-Phe-Leu-Leu-Arg-NH<sub>2</sub>: ES-MS  $m/z$  619.6 (MH<sup>+</sup>), <sup>1</sup>H NMR (400 MHz); (3) H<sub>2</sub>N-Ser- $\Psi$ (COO)-Phe-Leu-Leu-Arg-NH<sub>2</sub>: ES-MS  $m/z$  635.4 (MH<sup>+</sup>), <sup>1</sup>H NMR (300 MHz, DMSO-*d*<sub>6</sub>); (4) H<sub>2</sub>N-Ser-Phe- $\Psi$ (COO)-Leu-Leu-Arg-NH<sub>2</sub>: FAB-MS  $m/z$  635.5 (MH<sup>+</sup>), <sup>1</sup>H NMR (400 MHz, CD<sub>3</sub>OD); (5) H<sub>2</sub>N-Ser-Phe-Leu-Leu- $\Psi$ (COO)-Arg-NH<sub>2</sub>: ES-MS  $m/z$  635.4 (MH<sup>+</sup>), <sup>1</sup>H NMR (400 MHz, DMSO-*d*<sub>6</sub>).<sup>70</sup>

**General procedure for the preparation of  $\alpha$ -methyl-substituted peptides.** The peptides were prepared via solid-phase synthesis on the Rink-amide resin as described above for the depsipeptides. However, when coupling to the  $\alpha$ -methyl amino acid or the  $\alpha$ -methyl peptide on the solid phase, the BOP-Cl reaction was repeated to insure complete coupling, on account of increased steric hindrance.

#### Examples

**A. Synthesis of H<sub>2</sub>N-Ser-( $\alpha$ -Me)Phe-Leu-Leu-Arg-NH<sub>2</sub>.** Fmoc-arginine(PMC)-functionalized Rink-amide resin, prepared above, (1 g, 0.46 mmol) was placed in an hour-glass bubbler with 20% piperidine in DMF

(20 mL) and agitated (nitrogen) for 1 h at 23°C. The solution was drawn off and the resin was washed with DMF (4×), CH<sub>2</sub>Cl<sub>2</sub> (2×), and DMF (3×), then combined with Fmoc-Leu-OH (480 mg, 1.35 mmol), HOBT (200 mg, 1.35 mmol), and DIC (170 mg, 1.35 mmol) in DMF (20 mL) and agitated for 3 h. After washing, the steps of deprotection and coupling with Fmoc-Leu-OH were repeated, followed by deprotection with 20% piperidine in DMF (20 mL) for 1 h. The tripeptido-resin was washed with DMF (5×) and CH<sub>2</sub>Cl<sub>2</sub> (3×), dried under a nitrogen stream, and stored at 0°C. Half of this resin (0.50 g, 0.23 mmol) was combined with Fmoc-(*S*)-2-amino-2-methyl-3-phenylpropionic acid (0.44 g, 1 mmol), DMAP (0.25 g, 2 mmol) in CH<sub>2</sub>Cl<sub>2</sub> (25 mL) and BOP-Cl (0.26 g, 1 mmol) were added, and it was agitated for 5 h at 23°C with periodic replacement of the evaporated solvent. The solution was drained off and the resin was washed with CH<sub>2</sub>Cl<sub>2</sub> (4×), DMF (3×) and CH<sub>2</sub>Cl<sub>2</sub> (3×), then resubjected to the same reaction procedure to insure complete coupling. Removal of the Fmoc group with 20% piperidine in DMF (20 mL) was followed by washing with DMF (5×) and CH<sub>2</sub>Cl<sub>2</sub> (5×). The resin was combined with Fmoc-Ser(*t*-Bu)-OH (0.42 g, 1.1 mmol), DMAP (0.24 g, 2 mmol), and BOP-Cl (0.26 g, 1 mmol) in CH<sub>2</sub>Cl<sub>2</sub> (20 mL) and agitated at 23°C for 5 h. After washing, the resin was resubjected to the same reaction conditions, followed by washing with CH<sub>2</sub>Cl<sub>2</sub> (3×), DMF (3×), CH<sub>2</sub>Cl<sub>2</sub> (3×), and DMF (2×). The Fmoc group was removed with 20% piperidine in DMF (20 mL) and the resin was washed with DMF (3×) and CH<sub>2</sub>Cl<sub>2</sub> (3×) and dried under a nitrogen stream. TFA (99%, 25 mL) was added and the mixture agitated for 3 h; the red solution was collected and evaporated in vacuo to an oil, which was triturated with ether (25 mL) to obtain a white solid (90 mg). The crude peptide was purified by reverse-phase HPLC by using the Waters Bondapak C18 column (40×100 mm) and 0.16% TFA in acetonitrile: 0.2% TFA in water (30:70). The solution was evaporated in vacuo to a solid, which was dissolved in water. This aqueous solution was frozen and lyophilized to give the titled compound (24 mg). ES-MS *m/z* 648.6 (MH<sup>+</sup>); <sup>1</sup>H NMR (400 MHz, CD<sub>3</sub>OD) δ 0.89–1.00 (2 pairs of d, 12H), 1.48 (s, Me, 2.7H), 1.40–1.95 (m, 11H), 3.09 (d, *J* = 13.4 Hz, 1H), 3.18 (m, 3H), 3.89 (dd, *J* = 3.9, 11.1 Hz, 1H), 3.97 (m, 2H), 4.15 (m, 1H), 4.30–4.45 (m, 3H), 7.15–7.33 (m, 5H, arom.), 7.70 (d, exch. H), 7.80 (d, exch. H), 8.10 (d, exch. H). FAB-HRMS calcd for C<sub>31</sub>H<sub>53</sub>N<sub>9</sub>O<sub>6</sub> + H<sup>+</sup>, 648.4197; found, 648.4211.

**B. Other α-methyl-substituted peptides.** In the same manner, the following α-methyl peptides were prepared. (1) H<sub>2</sub>N-(α-Me)Ser-Phe-Leu-Leu-Arg-NH<sub>2</sub>: ES-MS *m/z* 648.6 (MH<sup>+</sup>), <sup>1</sup>H NMR (400 MHz, CD<sub>3</sub>OD); (2) H<sub>2</sub>N-Ser-Phe-(α-Me)Leu-Leu-Arg-NH<sub>2</sub>: ES-MS *m/z* 648.3 (MH<sup>+</sup>), <sup>1</sup>H NMR (300 MHz); (3) H<sub>2</sub>N-Ser-Phe-Leu-(α-Me)Leu-Arg-NH<sub>2</sub>: ES-MS *m/z* 648.6 (MH<sup>+</sup>), <sup>1</sup>H NMR (300 MHz); (4) H<sub>2</sub>N-Ser-Phe-Leu-Leu-(α-Me)Arg-NH<sub>2</sub>: FAB-MS *m/z* 648.7 (MH<sup>+</sup>), <sup>1</sup>H NMR (400 MHz, DMSO-*d*<sub>6</sub>).<sup>70</sup>

**Synthesis of Fmoc-(α-Me)-Phe-OH.**<sup>63</sup> Sodium carbonate (1.81 g, 17.07 mmol) was dissolved in water (30 mL)

and 1,4-dioxane (15 mL) was added. (*S*)-2-Amino-2-methyl-3-phenylpropionic acid (1.02 g, 5.69 mmol) was added and the solution was cooled to 0°C. 9-Fluorenylmethylchloroformate (1.47 g, 5.69 mmol) in 1,4-dioxane (15 mL) was added over 10 min and the solution was stirred at 0°C for 30 min, then at 23°C for 16 h. The reaction was diluted with water, extracted with ether (2×), and acidified with aqueous HCl (pH = 1). The milky solution was extracted with chloroform: 2-propanol (4:1, 2×). The organic solution was washed with brine (2×), dried (Na<sub>2</sub>SO<sub>4</sub>), and evaporated in vacuo to a clear oil (2.22 g), which was used without further purification. FABMS *m/z* 402.3 (MH<sup>+</sup>); <sup>1</sup>H NMR (300 MHz, DMSO-*d*<sub>6</sub>) δ 1.17 (s, Me), 2.93 (d, *J* = 13.1 Hz, 1H), 3.26 (d, *J* = 13.3 Hz, 1H), 4.25–4.40 (m, 2H), 4.51 (dd, *J* = 6.2, 10.2 Hz, 1H), 7.00–7.45 (m, 9H, arom.), 7.73 (d, *J* = 7.5 Hz, 2H), 7.91 (d, *J* = 7.3 Hz, 2H).

**Synthesis of Boc-Ser(Bz)-CHO.**<sup>65</sup> Triethylamine (1.58 g, 15.6 mmol) was added to Boc-serinol(OBz) (1.1 g, 3.9 mmol) in dry DMSO (10 mL) under argon, followed by slow addition (10 min) of a DMSO (15 mL) solution of sulfur trioxide:pyridine complex (2.5 g, 15.6 mmol) at 23°C. After stirring for 3 h, the reaction mixture was poured into water (300 mL) and extracted with ether (125 mL, 3×). The ether solution was washed with 10% citric acid (2×), water (2×), saturated NaHCO<sub>3</sub> (2×), then dried (MgSO<sub>4</sub>) and evaporated in vacuo to give a clear oil (1.04 g), which was used without further purification. ES-MS *m/z* 280.2 (MH<sup>+</sup>); <sup>1</sup>H NMR (300 MHz, CDCl<sub>3</sub>) δ 1.48 (s, Me, 9 H), 3.68 (dd, *J* = 12, 2.0 Hz; 1H), 4.0 (dd, *J* = 12, 1.5 Hz; 1H), 4.31 (m, 1H), 4.51 (br s, CH<sub>2</sub>Ph), 4.56 (m, CH), 7.22–7.40 (m, 5H, arom.), 9.65 (s, CHO).

**General procedure for the preparation of reduced-amide peptides.** These peptides were prepared on the MBHA resin by using a classical Boc protocol. A solution of TFA:CH<sub>2</sub>Cl<sub>2</sub> (1:1, 15 mL) containing DMS (2%) was used to deprotect the Boc group from the growing peptide (0.33 mmol) followed by CH<sub>2</sub>Cl<sub>2</sub> washing (6×), then a CH<sub>2</sub>Cl<sub>2</sub>:triethylamine (10:1, 15 mL) wash (2×), again followed by CH<sub>2</sub>Cl<sub>2</sub> washing (6×). Coupling with the next Boc-protected amino acid (1 mmol) was achieved with DIC (1 mmol) and HOBT (1 mmol) in DMF:CH<sub>2</sub>Cl<sub>2</sub> (1:1, 10 mL). Reductive amination of the amino peptide on resin with the Boc-protected L-amino aldehyde (1.33 mmol) employed the method of Sasaki and Coy<sup>71</sup> by using NaBH<sub>3</sub>CN (1.33 mmol) in DMF:DCE (1:2). The product was cleaved from the resin, along with side-chain deprotection, by using liquid HF: anisole (10:1) at 0°C for 4 h. After evaporation of the HF, the mixture was triturated with ether and the product was dissolved in methanol. The solution was evaporated to a white solid, which was purified by reverse-phase HPLC and lyophilized to afford desired target.

## Examples

**A. Synthesis of H<sub>2</sub>N-Ser-Phe-(CH<sub>2</sub>NH)-Leu-Leu-Arg-NH<sub>2</sub>.** MBHA resin (1 g, 0.66 mmol) was washed with CH<sub>2</sub>Cl<sub>2</sub> (15 mL, 2×) and combined with Boc-Arg(Mts)-OH (0.9 g, 2 mmol) and HOBT (0.31 g, 2 mmol) in

DMF:CH<sub>2</sub>Cl<sub>2</sub> (1:1, 30 mL). The DIC (0.25 g, 2 mmol) was added, the mixture was agitated for 2 h (negative ninhydrin test), and the solution was drained. The resin was washed with CH<sub>2</sub>Cl<sub>2</sub> (6×, 30 mL), deprotected by treating it twice with TFA:CH<sub>2</sub>Cl<sub>2</sub>:DMS (49:49:2, 30 mL, 2 min/30 min), washed with CH<sub>2</sub>Cl<sub>2</sub> (6×, 30 mL), washed twice with CH<sub>2</sub>Cl<sub>2</sub>:triethylamine (10:1, 30 mL, 2 min), and washed with CH<sub>2</sub>Cl<sub>2</sub> (6×, 30 mL). The resin was combined with Boc-Leu-OH (0.50 g, 2 mmol), and HOBT (0.31 g, 2 mmol) in DMF:CH<sub>2</sub>Cl<sub>2</sub> (1:1, 30 mL) followed by DIC (0.25 g, 2 mmol) and agitated for 2 h at 23°C. As above, the resin was washed, deprotected, washed, and resubjected to the same coupling conditions to add the second leucine. A portion of the resin (0.25 g, 0.165 mmol) was deprotected and washed as above and combined with Boc-Phe-CHO<sup>29</sup> (165 mg, 0.66 mmol) in DMF:DCE (1:2, 5 mL) containing 1% HOAc and agitated for 1 h. NaBH<sub>3</sub>CN (42 mg, 0.67 mmol) was added in small portions over the next 1 h and agitated at 23°C for 16 h. The solution was removed and the resin was washed with DMF (6×) and CH<sub>2</sub>Cl<sub>2</sub> (6×). The Boc group was cleaved in the usual manner and, following the washings, the resin was coupled to Boc-Ser-OH (102 mg, 0.5 mmol) with HOBT (79 mg, 0.5 mmol) and DIC (93 mg, 0.75 mmol) as above. The resin was washed with DMF (6×) and CH<sub>2</sub>Cl<sub>2</sub> (6×), and dried in vacuo. The resin was combined with liquid HF:anisole (10:1, 10 mL) at 0°C and stirred for 4 h. The HF was evaporated and the residue was diluted with ether (20 mL) and stored at 0°C for 16 h. The resin and solids were collected, mixed with methanol, and filtered. The filtrate was evaporated to a solid, which was purified by using the Bondapak C18 3.9×300 mm HPLC column with 0.16% TFA in acetonitrile:0.20% TFA in water (35:65) to yield the title compound (3.3 mg). ES-MS *m/z* 620.6 (MH<sup>+</sup>); <sup>1</sup>H NMR (300 MHz) δ 0.84 (d, *J*=6.0 Hz, 3H), 0.89 (d, *J*=6.0 Hz, 3H), 0.96 (m, 6H), 1.30–1.95 (m, 10H), 2.75–2.95 (m, 2H), 3.15 (m, 2H), 3.28 (dd, *J*=7.0, 7.0 Hz, 2H), 3.82–4.18 (m, 5H), 4.42 (dd, *J*=7.0, 7.0 Hz, 1H), 4.69 (dd, *J*=8.0, 8.0 Hz, 1H), 7.25–7.48 (m, 5H, arom.). FAB-HRMS calcd for C<sub>30</sub>H<sub>53</sub>N<sub>9</sub>O<sub>5</sub>+H<sup>+</sup>, 620.4248; found, 620.4218.

**B. Other reduced-amide peptides.** In the same manner, the following reduced-amide peptides were synthesized. (1) H<sub>2</sub>N-Ser-Ψ(CH<sub>2</sub>NH)-Phe-Leu-Leu-Arg-NH<sub>2</sub>: ES-MS *m/z* 620.5 (MH<sup>+</sup>), <sup>1</sup>H NMR (300 MHz); (2) H<sub>2</sub>N-Ser-Phe-Leu-Ψ(CH<sub>2</sub>NH)-Leu-Arg-NH<sub>2</sub>: ES-MS *m/z* 620.6 (MH<sup>+</sup>), <sup>1</sup>H NMR (300 MHz); (3) H<sub>2</sub>N-Ser-Phe-Leu-Leu-Ψ(CH<sub>2</sub>NH)-Arg-NH<sub>2</sub>: ES-MS *m/z* 620.6 (MH<sup>+</sup>), <sup>1</sup>H NMR (300 MHz).<sup>70</sup>

**Synthesis of H<sub>2</sub>N-Ser-Phe-(*cis*-2-aminocyclopentylcarboxy)-Leu-Arg-NH<sub>2</sub> (3).** The H<sub>2</sub>N-Leu-Arg(PMC)-functionalized Rink-amide resin (0.45 g, 0.2 mmol), prepared above, was placed in an hour-glass bubbler with dry CH<sub>2</sub>Cl<sub>2</sub> (20 mL), DMAP (171 mg, 1.45 mmol), and Fmoc-protected *cis*-2-amino-1-cyclopentanecarboxylic acid (245 mg, 0.7 mmol) and agitated while BOC-Cl (153, 0.6 mmol) was added. After 5 h, the solution was separated. The resin was washed [CH<sub>2</sub>Cl<sub>2</sub> (5×); DMF (5×)] and deprotected with 20% piperidine:DMF

(20 mL) for 1 h. The resin was washed [DMF (5×); CH<sub>2</sub>Cl<sub>2</sub> (5×)] and coupled with Fmoc-Phe-OH (426 mg, 1.1 mmol), DMAP (244 mg, 2 mmol) and BOP-Cl (255 mg, 1 mmol) in CH<sub>2</sub>Cl<sub>2</sub> (20 mL), as above. Deprotection of the Fmoc group and the washings were repeated. The final coupling was accomplished with Fmoc-Ser(O-*t*-Bu)-OH (230 mg, 0.6 mmol), HOBT (95 mg, 0.6 mmol), and DIC (76 mg, 0.6 mmol) in DMF (20 mL) for 3 h. The resin was washed with DMF (5×), deprotected with 20% piperidine:DMF (45 min), washed with DMF (5×) and CH<sub>2</sub>Cl<sub>2</sub> (5×), and dried in vacuo. The product was cleaved with TFA:anisole (99:1, 20 mL) and the collected solution was concentrated in vacuo to a residue, which was triturated with ether and dissolved in water (20 mL). This solution was frozen and lyophilized to white solid. The crude product was purified on a Bondapak C18 (3.9×300 mm) HPLC column with 0.16% TFA in acetonitrile:0.2% TFA in water (gradient: 10:90 to 80:20 over 40 min) as the eluant to give a white solid (38 mg). ES-MS *m/z* 632.6 (MH<sup>+</sup>); <sup>1</sup>H NMR (400 MHz, CD<sub>3</sub>OD) δ 0.92 (d, *J*=6.0 Hz, 3H), 0.95 (d, *J*=6.0 Hz, 3H), 1.30 (m, 1H), 1.48–1.96 (m, 12H), 2.94 (dd, *J*=8, 12 Hz, 1H), 3.0–3.25 (m, 3H), 4.22–4.48 (m, 6H), 4.60 (m, 1H), 7.22–7.40 (m, 5H, arom.). FAB-HRMS calcd for C<sub>30</sub>H<sub>49</sub>N<sub>9</sub>O<sub>6</sub>+H<sup>+</sup>, 632.3884; found, 632.3877.

**Synthesis of peptides 1, 2, 4, and 5.** These analogues were prepared the same manner as for 3. (1) H<sub>2</sub>N-Ser-Phe-(*cis*-3-aminocyclohexylcarboxy)-Leu-Arg-NH<sub>2</sub> (1) from Fmoc-protected *cis*-3-amino-1-cyclohexanecarboxylic acid [HPLC: Waters Bondapak C18 (40×100 mm), 0.16% TFA in acetonitrile:0.2% TFA in water (22:78)]; diastereomer A, *t*<sub>R</sub>=28.0–30.5 min, ES-MS *m/z* 646.3 (MH<sup>+</sup>), <sup>1</sup>H NMR (400 MHz); diastereomer B, *t*<sub>R</sub>=31.0–36.0 min, ES-MS *m/z* 646.3 (MH<sup>+</sup>), <sup>1</sup>H NMR (400 MHz).<sup>70</sup> (2) H<sub>2</sub>N-Ser-Phe-(*trans*-3-aminocyclohexyl-carboxy)-Leu-Arg-NH<sub>2</sub> (2) from Fmoc-protected *trans*-3-amino-1-cyclohexanecarboxylic acid<sup>72</sup> [HPLC: Waters Bondapak C18 (40×100 mm), 0.16% TFA in acetonitrile:0.2% TFA in water (25:75)]; diastereomer A, *t*<sub>R</sub>=20.5–24.0 min, ES-MS *m/z* 646.3 (MH<sup>+</sup>), <sup>1</sup>H NMR (400 MHz); diastereomer B, *t*<sub>R</sub>=37.2–41.1 min, ES-MS *m/z* 646.3 (MH<sup>+</sup>), <sup>1</sup>H NMR (400 MHz).<sup>70</sup> (3) H<sub>2</sub>N-Ser-Phe-(*trans*-2-aminocyclohexylcarboxy)-Leu-Arg-NH<sub>2</sub> (4) from Fmoc-protected *trans*-2-amino-1-cyclohexanecarboxylic acid: mixture of diastereomers, ES-MS *m/z* 646.6 (MH<sup>+</sup>), <sup>1</sup>H NMR (300 MHz).<sup>70</sup> (4) H<sub>2</sub>N-Ser-Phe-(*cis*-2-aminocyclohexylcarboxy)-Leu-Arg-NH<sub>2</sub> (5) from Fmoc-protected *cis*-2-amino-1-cyclohexanecarboxylic acid: diastereomer A, HPLC *t*<sub>R</sub>=17.0–18.5 min, ES-MS *m/z* 646.6 (MH<sup>+</sup>), <sup>1</sup>H NMR (300 MHz); diastereomer B, HPLC *t*<sub>R</sub>=21.0–22.5 min, ES-MS *m/z* 646.6 (MH<sup>+</sup>), <sup>1</sup>H NMR (300 MHz).<sup>70</sup>

**Gel-filtered platelet aggregation agonist activity.** Human platelet-rich plasma (PRP) concentrate (Biological Specialties, Inc) was gel filtered (Sephacrose 2B, Pharmacia) in Tyrode's buffer (140 mM NaCl, 2.7 mM KCl, 12 mM NaHCO<sub>3</sub>, 0.76 mM Na<sub>2</sub>HPO<sub>4</sub>, 5.5 mM dextrose, 5 mM Hepes, and 2 mg/ml bovine serum albumen at pH 7.4). The gel-filtered platelets were diluted with Tyrode's

buffer (143,000 platelets/ $\mu\text{L}$ , final platelet count per well) and 2 mM  $\text{CaCl}_2$  in a 96-well microtiter plate. Platelet aggregation was initiated by the addition of a fixed concentration of the test compound dissolved in buffer or by a concentration of human  $\alpha$ -thrombin (American Diagnostica) sufficient to achieve 80% aggregation (0.015–0.075 NIH units/mL). The assay plate was stirred constantly. Platelet aggregation was monitored by intermittently placing the plate in a microplate reader (Molecular Devices) to read optical density (650 nm, DSOF) at 0 and 5 min after thrombin addition. Aggregation was calculated to be the decrease in optical density between 0 and 5-min time measurements. The percentage aggregation for each test compound relative to thrombin was determined by dividing the aggregation of the test sample by the aggregation of thrombin (maximal response) and multiplying the result by 100. All samples were tested in duplicate wells on the same plate. For  $\text{EC}_{50}$  determinations, a percentage of aggregation relative to thrombin was used.

**Inhibition of gel-filtered platelet aggregation induced by thrombin.** Gel-filtered platelets (*vide supra*) were diluted with Tyrode's buffer (143,000 platelets/ $\mu\text{L}$ , final platelet count per well), compound solution in buffer, and 2 mM  $\text{CaCl}_2$  in a 96-well microtiter plate. Platelet aggregation was initiated by addition of a concentration of human  $\alpha$ -thrombin (American Diagnostica) sufficient to achieve 80% aggregation (0.015–0.075 NIH units/mL). The assay plate was stirred constantly. Platelet aggregation was monitored and calculated as described above. All samples were tested in duplicate wells on the same plate. The test compound was dissolved in DMSO at a concentration of 10 mM, diluted to the desired concentration with deionized water, and then added to the assay well containing platelets, prior to the initiation of aggregation by  $\alpha$ -thrombin. The percent inhibition of platelet aggregation was measured by comparing aggregation in the presence and absence of test compound; it was calculated using the following equation: % inhibition =  $100 - \{(\% \text{ aggregation with test compound} / \% \text{ aggregation without test compound}) \times 100\}$ .  $\text{IC}_{50}$  values are defined as the concentration of the test compound that results in 50% inhibition of platelet aggregation.

**Thrombin receptor (PAR-1) binding assay.**<sup>73</sup> The radioligand Ser-*p*FPhe-Har-Leu-Har-Lys-(<sup>3</sup>H-Tyr)-NH<sub>2</sub> was prepared by Amersham Pharmacia Biotech by catalytic tritiation of an iodotyrosyl-containing precursor to a specific activity level of 46 Ci/mmol. Binding assays were performed in 24-well plates in a final volume of 200  $\mu\text{L}$ . The assay buffer consisted of 50 mM Hepes pH 7.5, 5 mM  $\text{MgCl}_2$ , and 0.1% bovine serum albumin. The membranes of CHRF-288 megakaryocytic cells<sup>74–76</sup> (25 mg in 100  $\mu\text{L}$ ) were incubated with 10 nM of the radioligand and different concentrations ( $10^{-9}$  to  $10^{-4}$  M) of the various test compounds. The total binding was determined in the absence of test compounds and nonspecific binding was determined in the presence of unlabeled S-*p*FPhe-Har-L-Har-KY-NH<sub>2</sub> at 10  $\mu\text{M}$ . Incubations were carried out for 30 min at 23°C. Reactions were arrested by addition of 1 mL of cold 20 mM

Hepes/138 mM NaCl (pH 7.5) and immediate filtration on Whatman GF/C filters, followed by four washes in a Brandel harvester (Brandel, Gaithersburg, MD). Radioactivity bound to the membranes on the filters was measured in a scintillation counter. Specific binding was determined by subtraction of nonspecific binding from total binding. The GF/C filters were presoaked for 2–3 h in 10 mM Hepes containing 0.5% polyethylenimine and 0.1 M *N*-acetylglucosamine to reduce nonspecific binding. Competition binding data were analyzed by using the Prism software (GraphPad, San Diego, CA).

**Circular dichroism studies.** Spectra were obtained using a Jasco model J-710 instrument calibrated with a standard solution of ammonium *d*-(+)-camphorsulfonate at 192 nm. Spectra were measured from 250 to 190 nm at 0.2-nm intervals. A scan speed of 20 nm/min with a response time of 8 s was used. Two scans were accumulated per sample. The path length of the quartz cell was 0.1 cm. Samples were run at room temperature (23°C). The peptide concentration in samples ranged from 50 to 300  $\mu\text{M}$ . The solvent (pH 7.2 phosphate buffer/TFE) baseline was recorded and subtracted from sample spectra. The final concentration in phosphate buffer was 12.5 mM in all TFE/aqueous solution mixtures. Peptide molar ellipticity is expressed in  $[\Theta]$  (deg-cm<sup>2</sup>/dmol).

**Structural NMR studies.** Proton spectra were recorded at 600 MHz on a Bruker DMX 600 spectrometer. Samples were 5–8 mg peptide dissolved in 400  $\mu\text{L}$  of 100 mM sodium phosphate buffer, pH 3.8 and 400  $\mu\text{L}$  of 2,2,2-trifluoroethanol-*d*<sub>3</sub>. Spectra were referenced by the addition of a small amount of internal standard trimethylsilylpropanoate  $\delta$  0.00). Assignments were made using standard TOCSY (DIPSI-2 spin-lock) and NOESY experiments. These spectra were recorded at 0°C using presaturation to suppress the water peak. Spin-lock mix times were between 50 and 100 ms or less than 20 ms for observation of only vicinal coupling partners. Cross-relaxation mix times were between 100 and 400 ms.

**Computational methods.** Molecular structures were generated in a neutral form and calculations were conducted in vacuum with a dielectric constant of 1. For a typical run, all bonded potential force constants were scaled by 0.4, a quadratic potential was used for covalent bond interactions, and no coulomb potential was introduced. A given starting conformation was partially minimized and heated to 1000 K. This elevated temperature, coupled with force field modifications to facilitate bond rotations and atom “tunneling”, considerably randomized the peptide prior to quenching and regularization. Structures were selected every picosecond and quenched by successive minimizations, by using a combination of steepest descent and conjugate gradients methods. The quenched structures were regularized under a more complete force field (no re-scaling; Morse bond potential and cross-term potentials, but no coulombic potential). Finally each conformation was completely minimized with the complete force field

until the maximum derivative was less than 0.001 kcal/mol/Å. All calculations were carried out using the CVFF force field<sup>77</sup> as implemented in Insight II version 2.95 (Biosym Technologies, CA). Hierarchical cluster analysis (average linkage method) was carried out using the S-Plus package (MathSoft, Data Analysis Products Division, 1700 Westlake Ave. N., Suite 500, Seattle, WA 98109).

### Acknowledgements

We thank members of the spectroscopy group for scientific discussions and for making their facilities very accessible; the molecular modeling group (especially Dr. Harold Almond, Jr.) for hardware and software assistance; and Dr. William Hoekstra for advice and assistance.

### References and Notes

- Jackson, T. *Pharmac. Ther.* **1991**, *50*, 425.
- Strader, C. D.; Fong, T. M.; Tota, M. R.; Underwood, D.; Dixon, R. A. F. *Annu. Rev. Biochem.* **1994**, *63*, 101.
- Strader, C. D.; Fong, T. M.; Graziano, M. P.; Tota, M. R. *FASEB J.* **1995**, *9*, 745.
- Moereels, H.; Lewi, P. J.; Koymans, L. M. H.; Janssen, P. A. J. *Recept. Channels* **1996**, *4*, 19.
- Gudermann, T.; Nürnberg, B.; Schultz, G. *J. Mol. Med.* **1995**, *73*, 51.
- Trumpp-Kallmeyer, S.; Hoflack, J.; Bruinvels, A.; Hibert, M. *J. Med. Chem.* **1992**, *35*, 3448.
- Vu, T.-K. H.; Wheaton, V. I.; Hung, D. T.; Coughlin, S. R. *Cell* **1991**, *64*, 1057.
- Van Obberghen-Schilling, E.; Chambard, J.-C.; Vouret-Craviari, V.; Chen, Y.-H.; Grall, D.; Pouysségur, J. *Eur. J. Med. Chem.* **1995**, *30S*, 117.
- Dennington, P. M.; Berndt, M. C. *Clin. Exp. Pharmacol. Physiol.* **1994**, *21*, 349.
- Coughlin, S. R.; Scarborough, R. M.; Vu, T.-K. H.; Hung, D. T. *Cold Spring Harbor Symp. Quant. Biol.* **1992**, *57*, 149.
- Coughlin, S. R. *Thromb. Haemostasis* **1993**, *66*, 184.
- Coughlin, S. R. *Trends Cardiovasc. Med.* **1994**, *4*, 77.
- Ogletree, M. L.; Natarajan, S.; Seiler, S. M. *Persp. Drug Discov. Des.* **1994**, *1*, 527.
- Scarborough, R. M.; Naughton, M.; Teng, W.; Hung, D. T.; Rose, J.; Vu, T.-K. H.; Wheaton, V. I.; Turck, C. W.; Coughlin, S. R. *J. Biol. Chem.* **1992**, *267*, 13146.
- For PAR-2: Nystedt, S.; Emilsson, K.; Wahlestedt, C.; Sundelin, J. *Proc. Natl. Acad. Sci. USA* **1994**, *91*, 9208.
- For PAR-2: Nystedt, S.; Emilsson, K.; Larsson, A.-K.; Stroembeck, B.; Sundelin, J. *Eur. J. Biochem.* **1995**, *232*, 84.
- For PAR-2: Nystedt, S.; Larsson, A.-K.; Aberg, H.; Sundelin, J. *J. Biol. Chem.* **1995**, *270*, 5950.
- For PAR-3: Ishihara, H.; Connolly, A. J.; Zeng, D.; Kahn, M. L.; Zheng, Y. W.; Timmons, C.; Tram, T.; Coughlin, S. R. *Nature (London)* **1997**, *386*, 502.
- For PAR-4: Xu, W.-F.; Andersen, H.; Whitmore, T. E.; Presnell, S. R.; Yee, D. P.; Ching, A.; Gilbert, T.; Davie, E. W.; Foster, D. C. *Proc. Natl. Acad. Sci. USA* **1998**, *95*, 6642.
- Kahn, M. L.; Zheng, Y.-W.; Huang, W.; Bigornia, V.; Zeng, D.; Moff, S.; Farese, R. V., Jr.; Tam, C.; Coughlin, S. R. *Nature* **1998**, *394*, 690.
- Hui, K. Y.; Jakubowski, J. A.; Wyss, V. L.; Angleton, E. L. *Biochem. Biophys. Res. Commun.* **1992**, *184*, 790.
- Sabo, T.; Gurwitz, D.; Motola, L.; Brodt, P.; Barak, R.; Elhanaty, E. *Biochem. Biophys. Res. Commun.* **1992**, *188*, 604.
- Chao, B. H.; Kalkunte, S.; Maraganore, J. M.; Stone, S. R. *Biochemistry* **1992**, *31*, 6175.
- Vassallo, R. R., Jr.; Kieber-Emmons, T.; Cichowski, K.; Brass, L. F. *J. Biol. Chem.* **1992**, *267*, 6081.
- Feng, D.-M.; Veber, D. F.; Connolly, T. M.; Condra, C.; Tang, M.-J.; Nutt, R. F. *J. Med. Chem.* **1995**, *38*, 4125.
- Natarajan, S.; Reixinger, D.; Peluso, M.; Seiler, S. M. *Int. J. Pept. Protein Res.* **1995**, *45*, 145.
- Seiler, S. M.; Peluso, M.; Tuttle, J. G.; Pryor, K.; Klimas, C.; Matsueda, G. R.; Bernatowicz, M. S. *Mol. Pharmacol.* **1996**, *49*, 190.
- Shimamoto, T.; Tsuboi, H.; Kitajima, Y.; Miyazaki, T.; Oyama, Y.; Imajo, S.; Ishiguro, M. *Bioorg. Med. Chem. Lett.* **1995**, *5*, 2417.
- Nose, T.; Shimohigashi, Y.; Ohno, M.; Costa, T.; Shimizu, N.; Ogino, Y. *Biochem. Biophys. Res. Commun.* **1993**, *193*, 694.
- Scarborough, R. M., personal communication.
- Smith, K. J.; Trayer, I. P.; Grand, R. J. A. *Biochemistry* **1994**, *33*, 6063.
- Ceruso, M. Ph.D. thesis, State University of New York at Stony Brook, 1994.
- Oksenberg, D.; Scarborough, R. M., unpublished results.
- Marshall, G. R.; Bosshard H. E.; Eilers N. C.; Needleman P. In *Chemistry and Biology of Peptides*: Meienhofer, J., Ed.; Ann Arbor Science: Ann Arbor, MI, 1972, pp 571–578.
- Marshall, G. R.; Bosshard, H. E. *Circulation Res.* **1972**, *31* (suppl. 2), 143.
- Ramnarayan, K.; Chan, M. F.; Balaji, V. K.; Profeta, S., Jr.; Rao, S. N. *Int. J. Pept. Protein Res.* **1995**, *45*, 366.
- Note:** Incorporation of branched,  $\alpha,\alpha$ -dialkyl amino acids into a peptide tends to induce folded structures, such as  $3_{10}$ -helical,  $\alpha$ -helical, and  $\beta$ -turn conformations (Mutter, M. *Angew. Chem., Int. Ed. Engl.* **1985**, *24*, 639; Prasad, B. V. V.; Balaram, P. *CRC Critical Rev. Biochem.* **1984**, *16*, 307; Karle, I. L.; Balaram, P. *Biochemistry* **1990**, *29*, 6747; Di Blasio, B.; Pavone, V.; Lombardi, A.; Pedone, C.; Benedetti, E. *Biopolymers* **1993**, *33*, 1037; Wipf, P.; Heimgartner, H. *Helv. Chim. Acta* **1988**, *71*, 258; Wipf, P.; Kunz, R. W.; Prewer, R.; Heimgartner, H. *Helv. Chim. Acta* **1988**, *71*, 268).
- Pettitt, B. M.; Matsunaga, T.; Al-Obeidi, F.; Gehig, C.; Hruby, V. J.; Karplus, M. *Biophys. J.* **1991**, *60*, 1540.
- Bruccoleri, R. E.; Karplus, M. *Biopolymers* **1990**, *29*, 1847.
- Lewis, P. N.; Momany, F. A.; Scheraga, H. A. *Biochim. Biophys. Acta* **1973**, *303*, 211.
- Milner-White, E. J.; Ross, B. M.; Ismail, R.; Belhadj-Mostefa, K.; Poet, R. *J. Mol. Biol.* **1988**, *204*, 777.
- Vass, E.; Kurz, M.; Konat, R. K.; Hollosi, M. *Spectrochim. Acta, Part A* **1998**, *54A*, 773.
- Hagler, A. T.; Osguthorpe, D. J.; Dauber-Osguthorpe, P.; Hempel, J. C. *Science* **1985**, *227*, 1309.
- Toniolo, C.; Formaggio, F.; Crisma, M.; Schoemaker, H. E.; Kamphuis, J. *Tetrahedron: Asymmetry* **1994**, *5*, 507.
- Banerjee, A.; Ragothama, S. R.; Karle, I. S.; Balaram, P. *Biopolymers* **1996**, *39*, 279.
- Burgen, A. S. V.; Roberts, G. C. K.; Feeney, J. *Nature (London)* **1975**, *253*, 753.
- Silverman, R. B. *The Organic Chemistry of Drug Design and Drug Action*. Academic: New York, 1992, pp 71–74.
- Bernatowitz, M. S.; Kllimas, C. E.; Hartl, K. S.; Peluso, M.; Allegretto, N. J.; Seiler, S. M. *J. Med. Chem.* **1996**, *39*, 4879.
- Coller, B. S.; Ward, P.; Ceruso, M.; Scudder, L. E.; Springer, K.; Kutok, J.; Prestwich, G. D. *Biochemistry* **1992**, *31*, 11713.
- Boulanger, Y.; Khiat, A.; Chen, Y.; Gagnon, D.; Poitras, P.; St.-Pierre, S. *Int. J. Pept. Protein Res.* **1995**, *46*, 527.

51. Hudson, D.; Kenner, G.; Sharp, R.; Szelke, M. *Int. J. Pept. Protein Res.* **1979**, *14*, 177.
52. Dauber-Osguthorpe, P.; Campbell, M.; Osguthorpe, D. *Int. J. Pept. Protein Res.* **1991**, *38*, 357.
53. Masdouri, L.; Aubry, A.; Sakarellos, C.; Gomez, E.; Cung, M.; Marraud, M. *Int. J. Pept. Protein Res.* **1988**, *31*, 420.
54. Ghosh, P.; Amaya, M.; Mellins, E.; Wiley, D. C. *Nature (London)* **1995**, *378*, 457.
55. Swain, A. L.; Miller, M. M.; Green, J.; Rich, D. H.; Schneider, J.; Kent, S. B. H.; Wlodawer, A. *Proc. Natl. Acad. Sci. USA* **1990**, *87*, 8805.
56. Siligardi, G.; Drake, A. F. *Biopolymers* **1995**, *37*, 281.
57. Munoz, V.; Blanco, F. J.; Serrano, L. *Nature Struct. Biol.* **1995**, *2*, 380.
58. Matsoukas, J.; Hollenberg, M. D.; Mavromoustakos, T.; Panagiotopoulos, D.; Alexopoulos, K.; Yamdagni, R.; Wu, Q.; Moore, G. J. *J. Protein Chem.* **1997**, *16*, 113.
59. Matsoukas, J.; Panagiotopoulos, D.; Keramida, M.; Mavromoustakos, T.; Yamdagni, R.; Wu, Q.; Moore, G. J.; Saifeddine, M.; Hollenberg, M. D. *J. Med. Chem.* **1996**, *39*, 3585.
60. We have studied macrocyclic analogues of SFLLRN, with a cyclization linkage between the P1 and P6 or the P3 and P6 side chains, for PAR-1 agonist activity in platelet activation, and found that some compounds with the P3/P6 linkage exhibit PAR-1 agonist activity at the level of TRAP-6.<sup>61</sup>
61. McComsey, D. F.; Hecker, L. R.; Andrade-Gordon, P.; Addo, M. F.; Maryanoff, B. E. *Bioorg. Med. Chem. Lett.* **1999**, *9*, 255.
62. For example, we have observed an extended conformation for peptide recognition motifs in a 19-membered-ring macrocyclic environment during complexation of inhibitor ligands with human  $\alpha$ -thrombin. Cyclotheonamide A, a 19-membered-ring thrombin inhibitor peptide: Maryanoff, B. E.; Qiu, X.; Padmanabhan, K. P.; Tulinsky, A.; Almond, Jr., H. R.; Andrade-Gordon, P.; Greco, M. N.; Kauffman, J. A.; Nicolaou, K. C.; Liu, A.; Brungs, P. H.; Fusetani, N. *Proc. Natl. Acad. Sci. USA* **1993**, *90*, 8048. A synthetic 19-membered-ring thrombin inhibitor peptide: Greco, M. N.; Powell, E. T.; Hecker, L. R.; Andrade-Gordon, P.; Kauffman, J. A.; Lewis, J. M.; Ganesh, V.; Tulinsky, A.; Maryanoff, B. E. *Bioorg. Med. Chem. Lett.* **1996**, *6*, 2947.
63. Carpino, L. A.; Han, G. Y. *J. Org. Chem.* **1972**, *37*, 3404.
64. Roeske, R. W.; Tian, Z.; Edwards, P. *Int. J. Pept. Protein Res.* **1992**, *40*, 119.
65. Hamada, Y.; Shioiri, T. *Chem. Pharm. Bull.* **1982**, *30*, 1921.
66. Fields, G. B.; Noble, R. L. *Int. J. Pept. Protein Res.* **1990**, *35*, 161.
67. Atherton, E.; Logan, C. J.; Sheppard, R. C. *J. Chem. Soc., Perkin Trans.* **1981**, *1*, 538.
68. Penke, B.; Rivier, J. *J. Org. Chem.* **1987**, *52*, 1197.
69. Diaz-Meseguer, J.; Palomo-Coll, A. L.; Fernandez-Lizarbe, J. R.; Zugaza-Bilbao, A. *Synthesis* **1980**, 547.
70. <sup>1</sup>H NMR data indicated a homogeneous material and supported the assigned structure; spectra are available on request to the corresponding author.
71. Sasaki, Y.; Coy, D. H. *Peptides* **1987**, *8*, 119.
72. Hewgill, F. R.; Jefferies, P. R. *J. Chem. Soc.* **1955**, 2767.
73. This PAR-1 binding assay was developed in our laboratories. For other PAR-1 binding assays, see: ref 25; Ahn, H.-S.; Foster, C.; Boykow, G.; Arik, L.; Smith-Torhan, A.; Hesk, D.; Chatterjee, M. *Molec. Pharmacol.* **1997**, *51*, 350.
74. Jones, C. L. A.; Witte, D. P.; Feller, M. J.; Fugman, D. A.; Dorn II, G. W.; Lieberman, M. A. *Biochim. Biophys. Acta* **1992**, *1136*, 272.
75. Fugman, D. A.; Witte, D. P.; Jones, C. L. A.; Aronow, B. J.; Lieberman, M. A. *Blood* **1990**, *75*, 1252.
76. Witte, D. P.; Stambrook, P. J.; Feliciano, E.; Jones, C. L. A.; Lieberman, M. A. *J. Cell. Physiol.* **1988**, *137*, 86.
77. Hagler, A. T.; Dauber, P.; Lifson, S. *J. Am. Chem. Soc.* **1979**, *101*, 5131.